A Critical Study of Cu2O: Synthesis and Its Application in CO2 Reduction by Photochemical and Electrochemical Approaches

Mohan, Sathya

Honnappa, Brahmari

Augustin, Ashil

Shanmugam, Mariyappan

他

出版情報：Catalysts. 12 (4), pp.445-, 2022-04-17. Multidisciplinary Digital Publishing Institute (MDPI)
バージョン：

catalysts

MDPI

Review

A Critical Study of Cu_2O: Synthesis and Its Application in CO_2 Reduction by Photochemical and Electrochemical Approaches

Sathya Mohan [1,†], Brahmari Honnappa [2,†], Ashil Augustin [1], Mariyappan Shanmugam [1], Chitiphon Chuaicham [3], Keiko Sasaki [3], Boopathy Ramasamy [4,*] and Karthikeyan Sekar [1,*]

1 Sustainable Energy and Environmental Research Laboratory, Department of Chemistry, SRM Institute of Science and Technology, Kattankulathur 603203, Tamil Nadu, India; sm0044@srmist.edu.in (S.M.); aa6663@srmist.edu.in (A.A.); ms8419@srmist.edu.in (M.S.)
2 Sustainable Energy & Environmental Research Laboratory, Department of Physics and Nanotechnology, SRM Institute of Science and Technology, Kattankulathur 603203, Tamil Nadu, India; bh0908@srmist.edu.in
3 Department of Earth Resources Engineering, Kyushu University, Fukuoka 819-0395, Japan; chitiphon.c@gmail.com (C.C.); keikos@mine.kyushu-u.ac.jp (K.S.)
4 Environment & Sustainability Department, Institute of Minerals and Materials Technology (CSIR-IMMT), Bhubaneswar 751013, Odisha, India
* Correspondence: boopathy@immt.res.in (B.R.); karthiks13@srmist.edu.in (K.S.)
† These authors contributed equally to this work.

Abstract: Copper oxide (Cu_2O) is a potential material as a catalyst for CO_2 reduction. Cu_2O nanostructures have many advantages, including interfacial charge separation and transportation, enhanced surface area, quantum efficiency, and feasibility of modification via composite development or integration of the favorable surface functional groups. We cover the current advancements in the synthesis of Cu_2O nanomaterials in various morphological dimensions and their photochemical and electrochemical applications, which complies with the physical enrichment of their enhanced activity in every application they are employed in. The scope of fresh designs, namely composites or the hierarchy of copper oxide nanostructures, and various ways to improve CO_2 reduction performance are also discussed in this review. Photochemical and electrochemical CO_2 transformations have received tremendous attention in the last few years, thanks to the growing interest in renewable sources of energy and green facile chemistry. The current review provides an idea of current photochemical and electrochemical carbon dioxide fixing techniques by using Cu_2O-based materials. Carboxylation and carboxylative cyclization, yield valuable chemicals such as carboxylic acids and heterocyclic compounds. Radical ions, which are induced by photo- and electrochemical reactions, as well as other high-energy organic molecules, are regarded as essential mid-products in photochemical and electrochemical reactions with CO_2. It has also been claimed that CO_2 can be activated to form radical anions.

Keywords: copper oxide (Cu_2O); CO_2 reduction; photochemical; electrochemical; nanostructures

Citation: Mohan, S.; Honnappa, B.; Augustin, A.; Shanmugam, M.; Chuaicham, C.; Sasaki, K.; Ramasamy, B.; Sekar, K. A Critical Study of Cu_2O: Synthesis and Its Application in CO_2 Reduction by Photochemical and Electrochemical Approaches. *Catalysts* **2022**, *12*, 445. https://doi.org/10.3390/catal12040445

Academic Editor: Anna Kubacka

Received: 22 March 2022
Accepted: 14 April 2022
Published: 17 April 2022

1. Introduction

Global warming and numerous health problems are caused by anthropogenic carbon dioxide (CO_2) emissions from excessive consumption of industrial-scale fossil fuels, which has an impact on the ecological and physiological viability. The atmospheric CO_2 level has risen from 280 ppm to >400 ppm over the last century, and it is anticipated to reach 700 ppm by the time a new century begins [1]. To maintain an environmentally friendly atmosphere while fulfilling fuel consumption and chemical demands, excess CO_2 has to be discarded or converted into a valuable resource. Climate change, fueled by historically high quantities of carbon dioxide in the atmosphere, is one of our society's most pressing issues. As part of a closed carbon cycle, photochemical and electrochemical CO_2 reduction has been proposed as a possible approach for producing useful hydrocarbon fuels (for example, as a means of storing renewable energy) that can be consumed without increasing the overall quantity

of CO_2 in the atmosphere. The rapidly growing exigency for fuels like hydrogen and other energy sources has become an immediate issue that needs to be resolved, as the world's economy and society evolve. Despite significant progress in the research growth in energy sources which are green and renewable, namely wave power, solar power, and hydropower, fossil energy remains the primary source of societal energy, accounting for more than 80% of total supply [2]. According to research published in Nature Climate Change, India's percentage of carbon dioxide (CO_2) emissions climbed more slowly from 2016–2019 than from 2011–2015, but were still much higher than the global average of 0.7% [3]. According to the National Oceanic and Atmospheric Administration (NOAA), there has been an increase to 382 ppm from 280 ppm in atmospheric CO_2 concentrations (ACC) level from pre-industrial times up until 2016. CO_2 concentration in our atmosphere is currently increasing at a rate of roughly 1.9 ppm each year. In line with this, the International Energy Outlook (2011) forecasts a 53% rise in global energy use from 2008 to 2035 [4]. CO_2 must be caught and either stored or transformed into global warming-neutral effect molecules to achieve this goal. CO_2 utilization is an appealing option for achieving this goal. Because carbon dioxide is a stable molecule both in terms of kinetics and thermodynamics, the process of converting CO_2 requires a high yielding catalyst and the process is endothermic as well. Various renewable energy sources, such as solar, wind, and hydropower, have been proposed as CO_2-conversion energy sources. These kinetic energies, which are mostly intermittent, are stored in alternate fuels as chemical energy, which can be transported and utilized on demand. These synthetic fuels will help to sustain new and increasing transportation markets. Furthermore, CO_2-derived synthetic fuels are compatible with present hydrocarbon-based transportation networks. Chemical, pharmaceutical, and polymer companies can use carbon dioxide conversion products as a way of supplementing or replacing chemical feedstocks [5].

The widespread employment of fossil fuels results in a vast volume of CO_2 gas being released into the atmosphere, causing uncontrollable harm to the environment. Photochemical and electrochemical reduction of CO_2 into organic energy molecules or other industrial-based raw materials are the key methods for lowering CO_2 levels in and around the environment and establishing a novel carbon resource balancing system. Nevertheless, due to a number of major issues, namely increased overpotential, lower selectivity, and expensive cost, the presently utilized catalysts for electrochemical and photochemical CO_2 reduction are even now inadequate [6]. The possibility of carbon contamination is a crucial issue that requires special consideration in CO_2-reduction studies. Organic substances used in catalyst preparation, such as solvents, reactants, and surfactants, may leave carbon-rich residues in the resultant product, which may decay into smaller molecules like carbon monoxide and methane during electrocatalysis or photocatalysis (particularly the latter), leading to an overestimation of catalytic activities [7]. Various hydrocarbon from CO2 reduction obtained can be expressed generally as [8]

$$x\mathrm{CO_2} + \mathrm{y}\left(\mathrm{H^+} + \mathrm{e^-}\right) \overset{\text{yields}}{\rightarrow} \mathrm{C}_x\mathrm{H}_{y-2n}\mathrm{O}_{2x-n} + n\mathrm{H_2}. \quad (1)$$

The electrons should possess excessive free energy or chemical potential to fuel the reaction. In photochemical and electrochemical carbon dioxide reduction reactions, the electrons' energy can be controlled by the conduction band and/or an applied potential edge, respectively [9]. Furthermore, in spite of the presence of catalysts, these reactions are unable to provide information about the kinetics of the reduction of CO_2, and are typically slow. The CO^{2-} anionic radical intermediate preparatory process is thought to be the initial step in the reduction of carbon dioxide. It can furthermore be lowered by protonating the oxygen or carbon atoms, resulting in COOH or HCOO [10].

Hori and coworkers [11] explored the fact that Au foils have the ability to convert CO_2 to CO, which has been an important component in the process of CO_2 reduction. This reaction is interesting because it could be a part of the carbon energy cycle. Hydrocarbon preparation from carbon dioxide involves several steps at the time of reaction, which include adsorbed intermediates and most importantly adsorbed carbon monoxide. Watanabe et al. [12], in 1991

published an analysis of Cu–M alloys, (M = Ag, Cd, Ni, Pb, Sn, and Zn); this was the first study of alloys for electrochemical CO_2 reduction. The copper–nickel alloy (Cu/Ni 90:10) was the most notable, suppressing CO generation in favor of methanol at a peak Faradaic efficiency of 7% at −0.9 V vs. the standard hydrogen electrode.

Cu and Ni have a synergistic effect, according to their findings. This deviation from linear scaling relations has now been identified as the result of a combination of two effects: the electronic impact, which alters the binding environment for intermediates, and the geometric effect, which alters the atoms arrangement at the active site [13].

To counter these effects, the photochemical CO_2 reduction is the generation of carrier charges, separation, transportation, and finally reduction of CO_2 utilizing produced photoelectrons in the photochemical transformation of CO_2. Photocatalytic carbon dioxide reduction is a burgeoning field of study.

In this review paper, we have discussed an outline of current developments in the synthetic process of copper oxide (Cu_2O) as a catalyst in photocatalytic and electrocatalytic CO_2 reduction. Given the recent upshifted research activities and increasingly profound ideology of these two processes of photocatalytic process for the generation of carrier charges, separation, transportation, and finally reduction of CO_2 by utilizing produced photoelectrons are all steps in the photochemical transformation of CO_2 and when turning CO_2 into its reduced form, electrochemical reduction is presented with their current status as visualized in Scheme 1 with the last 6 years progress in photocatalytic and electrocatalytic CO_2 reduction [14–25]. Despite the fact that the two approaches use different experimental procedures, the goal is the same: to activate the carbon dioxide molecule, which is inert in terms of chemical properties, and increase its productive conversion in response to external energy stimuli. Furthermore, in photocatalytic and electrochemical processes, the surface charge transfer step that could be improved by using appropriate catalysts and good co-catalysts. This is why we believe photocatalytic CO_2 reduction and electrocatalytic CO_2 reduction are inextricably linked and have chosen to explore them jointly in our work. The review attempts to extensively study the synthesis of various dimensional Cu_2O structures continued with its application in photochemical and electrochemical carbon dioxide reduction into value-added products.

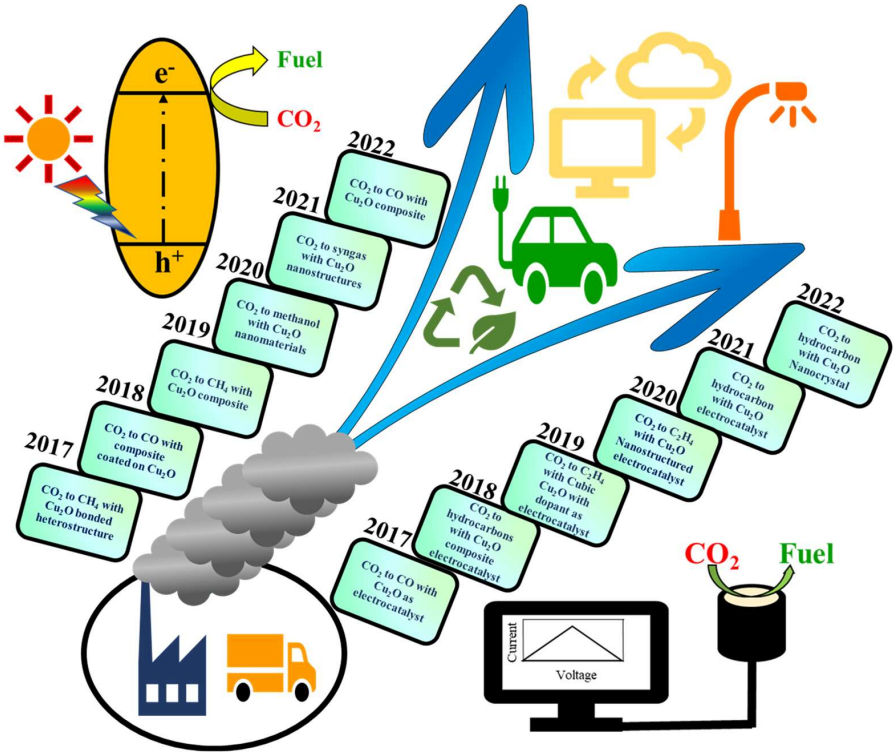

Scheme 1. Schematic representation of recent trends in Cu_2O as an efficient photo- and electrocatalyst for CO_2 reduction [14–25].

2. Synthesis of Cu_2O

Transition metal oxides are a kind of semiconductor used in magnetic storage, solar energy conversion, electronics, and catalysis. The various methods of synthesis of the catalyst Cu_2O are discussed as follows.

2.1. Synthesis of Cu_2O Material in Zero-Dimension

Low dimensional structures like quantum dots have received more attention due to the nanometer-sized (2–10 nm) offering high surface area so that it has a high active site. It is a semiconductor nanoparticle with various types of quantum dots available such as group transition-metal dichalcogenides, perovskites, carbon, and II-VI and I–III-VI compounds [26]. Among these, Cu_2O has a great interest because of the electronic arrangements and the significant binding energy of the exciton (140 meV), a very well-defined succession of excitonic characteristics may be observed in the luminescence and absorption spectra at minimum temperatures. It is a p-type semiconductor with wide application in the photocatalysis field. Yin et al. [27] in 2005 synthesized Cu_2O nanocrystals by using a novel and simple wet chemical method (Figure 1) in which the reaction size is decreased if copper and the oleic acid ratios were increased.

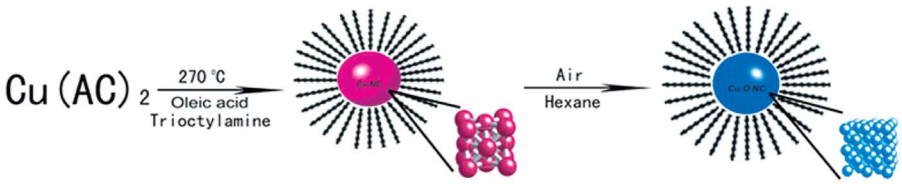

Figure 1. Graphical representation of the synthesis of Cu_2O quantum dot. [27] Copyright American Chemical Society, 2005.

Borgohain et al. [28], in 2002 synthesized the quantum size (2 nm) of Cu_2O by the electrochemical method. In this reaction anode material was copper electrode, the cathode was platinum and the electrolyte solution was a 4:1 ratio of acetonitrile and tetrahydrofuran. The resulting product was green in color and found when the increasing current density size was decreased. Nguyen et al. [29], in 2017 synthesized a novel composite based on Cu_2O quantum dot by hydrothermal method. A Cu_2O quantum dot/graphene-TiO_2 composite was used for photo degradation of rhodamine B, reactive black B, and methylene blue. Wenquan et al. [30], in 2014 reported the photocatalytic organic dyes and phenol degradation by Cu_2O quantum dot incorporated BiOBr. The main advantage is that upon incorporation, degradation efficiency was increased by 12 times.

2.2. Synthesis of One-Dimensional Cu_2O

One-dimensional (1D) metal oxides have grabbed tremendous attention in the last few years due to their distinguished properties and their profound potential use in a variety of fields. On the other hand, synthesizing a small size of 1D material is difficult. Several forms of 1D material are available such as nanowire, nanorod, nanotube, nanofiber, nanofilaments, and nanoplates.

Cu_2O is getting more attention, because it possesses enormous application in various nanodevices. One-dimensional, semi-conducting, nanoscale materials are said to offer a variety of fascinating physical features and uses, such as ultra-low-power nanowire light-emitting devices. For example, a cuprous oxide is currently attracting a lot of attention because excitons may travel coherently through monocrystalline Cu_2O samples, which is a p-type semiconductor having a bandgap value of ~2 eV. Changzheng Wu et al. [31], in 2003, synthesized monocrystalline Cu_2O nanowires by using a unique complex-precursor surfactant-assisted method, wherein the copper cations are aligned linearly in Cu_3 $(dmg)_2Cl_4$ and act as precursors for Cu_2O nanowire development. Several complicated nanorod-based structures have been synthesized thus far, including multi-armed, dendritic, self-sustained, and penniform structures. Cu_2O nanorod-based structures

were developed in a water–toluene system employing salicylaldehyde as the reducing agent and ligand, and an interface etching approach was carried out (Figure 2a–d) as observed showing various morphology [32].

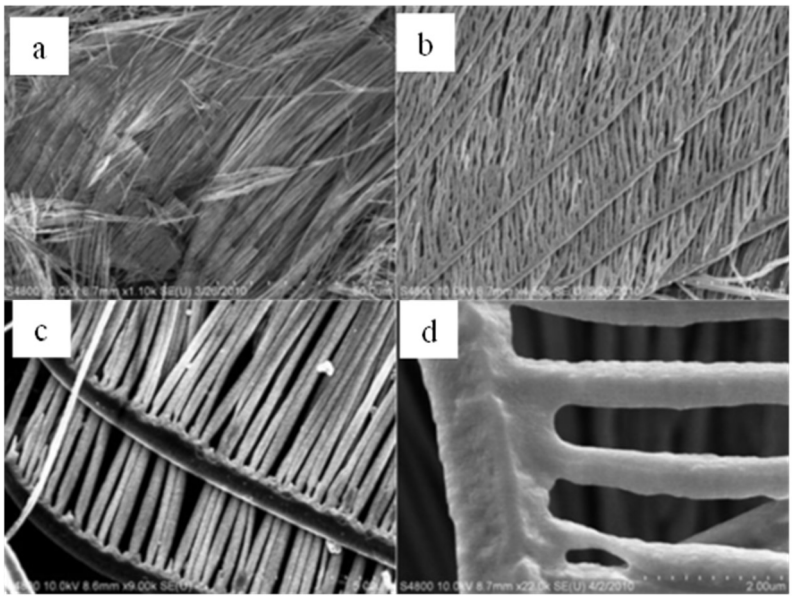

Figure 2. Scanning electron microscopic (SEM) image-comb-like Cu_2O nanorod with different magnifications (**a**–**d**). Reproduced with permission from [32]. Copyright The Royal Society, 2010.

Ying Yu et al. [33], in 2011 established the chemical bath deposition (CBD) procedure, which tunes the deposition of a thin coating by precipitation by using a controlled chemical reaction. Cu_2O nanorod thin films have been produced satisfactorily on Ti foil, fluorine-doped tin oxide glass, and Cu foil by utilizing the chemical bath deposition approach, employing cetrimonium bromide (CTAB). CTAB, a surfactant, is known to be important in the creation of nanorod shapes. In 2018, Rui Chen et al. [34] synthesized 1D Cu_2O with a template-free microwave-assisted method. Surfactants were not utilized to stimulate growth in this procedure, and the reaction took less time. XRD, EDS, and HRTEM investigations confirmed the production of Cu_2O nanowires (Figure 3a) and based on the morphological evolutions, a plausible growth mechanism was proposed (Figure 3b). The irradiation of microwave energy into the Cu_2O initial particles developed radially into nanowires in a series of time-dependent tests. The condition-variable experiments demonstrated that the right amount of NaOH addition was crucial for the creation of Cu_2O nanowires. The sample's photocatalytic property was studied by using visible light at room temperature for degradation of methyl orange. The prepared catalyst, could destroy 73% of methyl orange in 120 min, owing to its high surface area.

By using a surfactant, CTAB, as the template, Fei et al. [35], in 2004 developed 1D Cu_2O nanowhiskers (Figure 4) possessing diameters of 15–30 nm by using a liquid deposition process at 25 °C. The nanowhiskers have a well-ordered crystallized 1D structure with the length of more than 200 nm, as shown by TEM and HRTEM, and the nanowhiskers grow mostly in (111) direction. Furthermore, the nano-whiskers have a large number of pores, that form an advantageous path for visible light driven photocatalysis. The 1D structure cannot be formed by using polyethylene glycol (PEG), glucose, or sodium dodecyl sulfate (SDS) as templates. CTAB reacts with small copper hydroxide which tends to absorb the hydroxy ions and becomes negatively charged, in order to disperse the very small particles of Cu $(OH)_2$ solids and enhances the augmentation of Cu_2O towards 1D path. This is in accordance with the TEM images of the compound taken at various stages of th reaction in developing Cu_2O nanowhiskers. In spite of CTAB being necessary for the synthesis of 1D

nanomaterials, the ionic behavior of the precursor is also important because Cu^{2+} does not produce nanowhiskers.

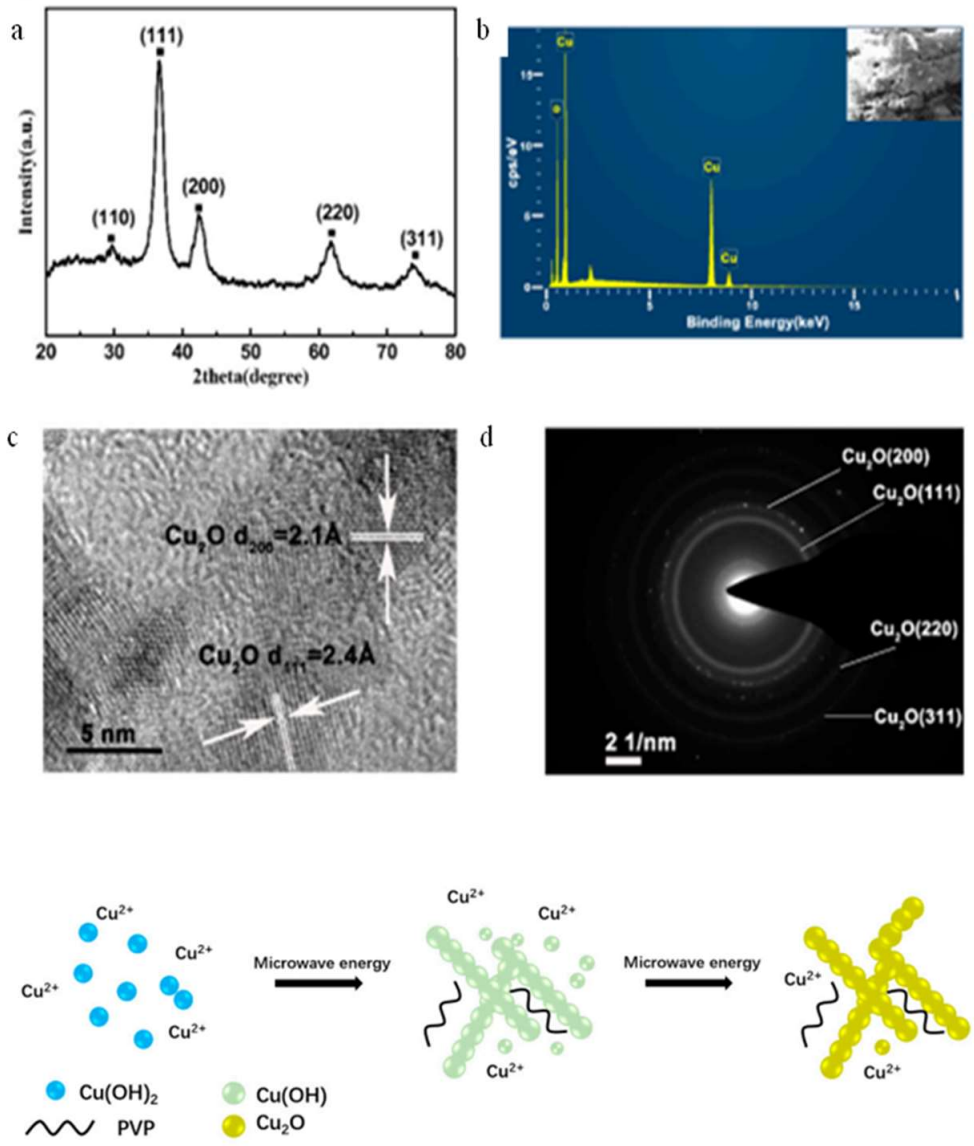

Figure 3. (**a**) X-Ray Diffraction pattern, (**b**) Energy-dispersive X-ray mapping, (**c**) High resolution-transmission electron microscope, (**d**) selected area energy diffraction pattern of synthesized 1D Cu_2O and the graphical representation for synthesizing 1D Cu_2O [34].

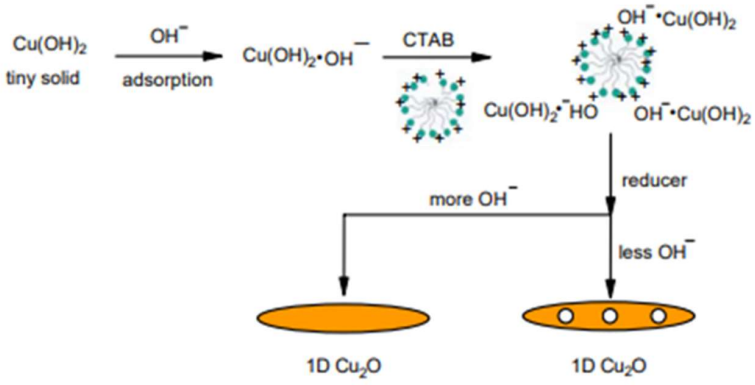

Figure 4. Schematic representation synthesis of Cu_2O whiskers [35]. Copyright Elsevier B.V., 2004.

At room temperature, Cu_2O nanowhiskers were successfully produced by Xinyong et al. [36] in 2008 by employing a unique wet chemical approach (Figure 5) involving polyethylene glycol as a surfactant and hydrazine as a reducing agent. X-ray diffraction (XRD), transmission electron microscope (TEM), UV-visible spectrophotometer and scanning electron microscope (SEM) were used to analyze the products. We discovered that the role of PEG for inducing Cu_2O development along the 1D direction is significantly relied upon by looking at SEM pictures of the obtained resultants. The production mechanism of the Cu_2O nanowhiskers was obtained.

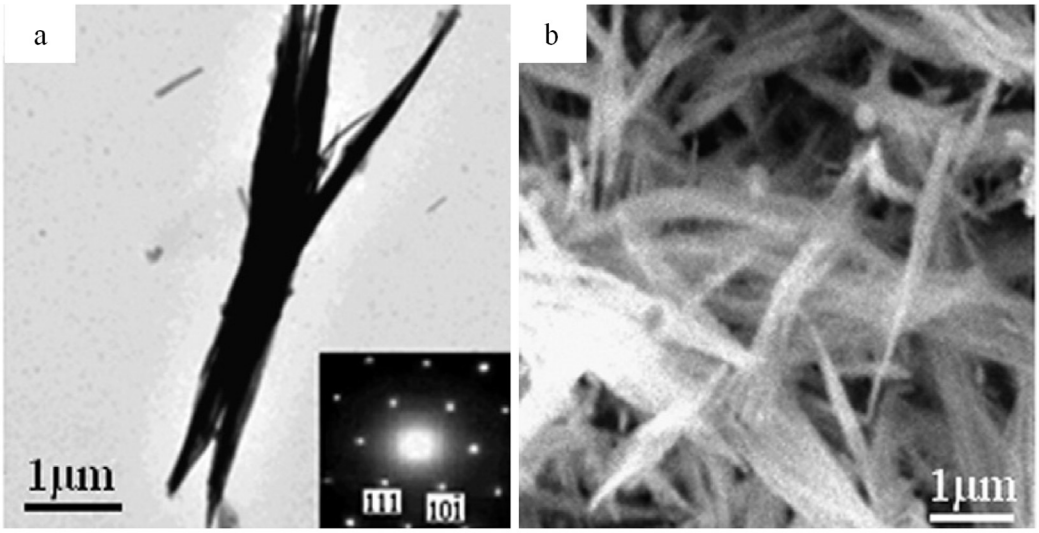

Figure 5. (**a**) Transmission electron microscope (TEM) image and (**b**) scanning electron microscope (SEM) image of Cu_2O nanowhiskers [36]. Copyright Elsevier B.V., 2008.

2.3. Synthesis of Cu_2O Two-Dimension

Peculiarly exposed surface features of two-dimensional (2D) nanomaterials imply excellent electron mobility and good thermal conductivity. Electron diffusion is greatly quickened, and electrochemically active sites are substantial in the case of 2D materials (Figure 6a,b) [37]. Due to their nanoscale thickness, 2D nanosheets are a potential nanomaterial with interlayer pores, and in-plane lattice. Depending on the molecule size, 2D nanosheets offer reduced transport resistance and increased selectivity [38]. The electrochemical features of nanosheets, such as high capacitance and low resistance, were found to be appealing. Due to the enhanced surface to volume ratio, 2D Cu_2O nanosheets do have larger specific surface area and enhanced active sites that are used for charge adsorption and storage.

Two-dimensional nanosheets offer the most stable morphological stability in terms of electrocatalytic activity. The high electrocatalytic activity of these nanosheets is due to their shortened ion and electron diffusion pathways. In addition to this, 2D nanosheets are said to have large numbers of electrochemical active sites with enhanced structural stability. Two-dimensional nanosheets are capable of forming bundles of nanosheets that are formed by self-aggregation in order to minimize the overall surface energy. Sambhaji M. Pawar et al. [39] in 2017 synthesized a highly efficient 2D copper oxide electrocatalyst by using the chemical bath deposition method. The Cu_2O electrode is said to be self-assembled on the substrate made up of stainless steel through a chemical bath deposition method followed by the air-annealing technique and is known to produce a 2D nanosheet bundle-type morphology. In 2016, Sonia Matencio et al. [40] used a scalable technology of air-enhanced argon sputtering with annealing. The team reported a novel honeycomb morphology of copper oxide possessing larger unit cells. In 2016, Kuibo Yin et al. [41] designed the fabrication of copper oxide possessing a square lattice with the thickness of a single atom. Monolayer oxides are an exceptionally fascinating type of 2D crystal because

of the multiple associated degrees of freedom inherent in bulk oxides (charge, spin, and lattice) with quantum confinement. In 2021, Suhyun Lee et al. [42] reported the synthesis of 2D copper nanosheets, which involved the green synthesis method that makes use of methylsulfonylmethane ($DMSO_2$) employing the Erlenmeyer flask in order to maintain the reaction temperature steadily for about 2 h. Wesley Luc et al. [43] in 2019 reported the synthesis of a 2D copper nanosheet by chemically reducing Cu (II) nitrate by the use of L-ascorbic acid by cetyltrimethylammonium bromide (CTAB) and hexamethylenetetramine (HMTA). They have fabricated a 2D nanosheet with a triangular-shaped morphology by utilizing the solution-phase synthesis procedure. Manab Mallik et al. [44] in 2020 reported a facile synthesis methodology of Cu_2O nanoparticles by the aqueous precipitation method which has its application in the synthesis of low-cost conductive ink. The preparation involved the use of copper sulfate and ascorbic acid in addition to PEG dissolved in deionized water. After consequent stirring and addition of sodium borohydride, a dark red solution was made. This solution after overnight cooling appeared to be yellow in colour and thus was separated by the centrifugation separation route (Figure 7).

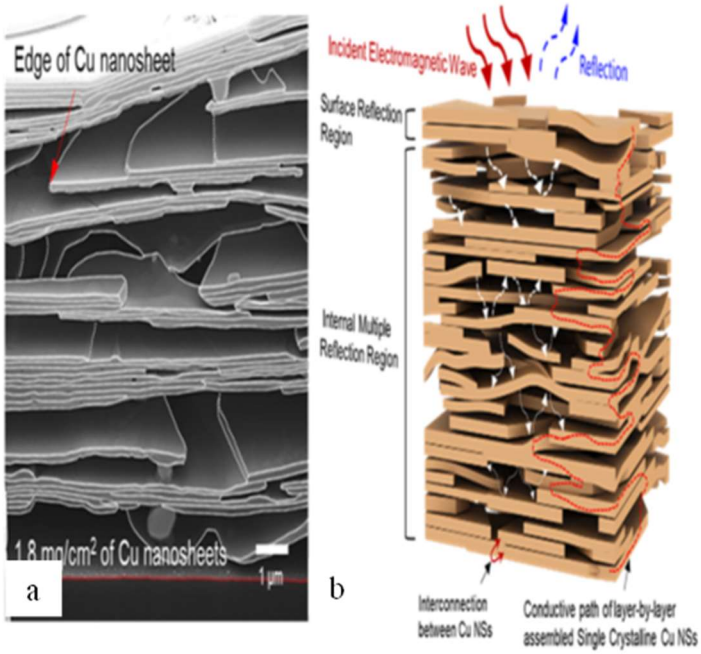

Figure 6. (**a**) Scanning electron microscope (SEM) image—copper oxide nanosheets. (**b**) Overlaid Cu nanosheets piled together. Reproduced with permission from [37]. Copyright American Chemical Society, 2021.

According to the production method of 2D copper oxide by transformation assembly of 1D copper hydroxide, the nanoleaf is an assembly of 1D nanowires. After removing oxygen from the copper oxide lattice and being reduced to copper, the spent catalyst takes on a sphere-like form [45]. Nanoleaves that are developed by one-step facile method offer an ideal catalyst for the oxidative degradation of methylene orange dye, which thus eliminates the need of heating and sunlight. Bhattacharjee et al. [46] in 2016 reported the facile green synthesis methodology for 2D copper oxide nanoleaves by using aspartic acid (amino acid) in the presence of sodium hydroxide by a microwave heating method. The use of amino acid in this method is to act as capping agent for the synthesis of copper oxide nanoleaves.

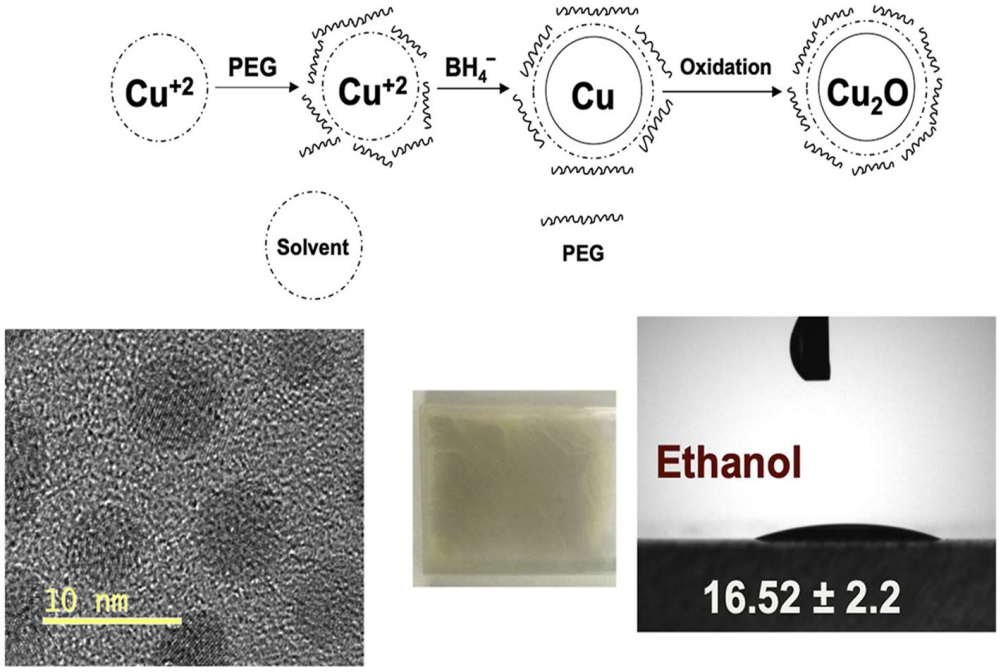

Figure 7. Illustration of Cu_2O synthesis methodology from Cu^{2+}. Reproduced with permission form [44]. Copyrights Elsevier B.V., 2021.

2.4. Synthesis of Three-Dimensional Cu_2O

Copper oxide, which is a p-type semiconductor, is of interest in the fields of rechargeable batteries, photocatalysis, catalysis, photo-detector, solar fuels, and chemical sensing, which is primarily due to its multi-functional capacity, and its high abundance, as it is found directly in nature and has a good response to the abovementioned applications [47]. With regard to its electrochemical aspects, the 3D copper oxide nanoflowers are vitally known to stimulate the diffusion of electrolytes at a much higher rate and create more channels for the diffusion of ions, which in turn leads to the enhanced performance of the electrode material [48].

Liutao Yu et al.in 2013 [49] successfully figured out a very simple yet effective wet chemical process to prepare the 3D porous gearlike structure which resemble the morphology of those nanoflowers found in 3D copper oxide. The synthesized material is said to possess high surface area, and hence it is available for a longer time to serve as a potent electrode in electrical energy storage (Figure 8). Xiang Fei et al. [50] in 2013, reported a facile one-pot synthesis methodology by employing silk fibron as a template in the preparation of hierarchical copper oxide nanoparticles, and the reaction is said to be carried out at room temperature. The final reaction was allowed to run at room temperature for about 5 days, and the resultant black precipitate is the 3D copper oxide nanoparticles possessing almond-like morphology (Figure 9). S.K. Shinde et al. [51] in 2014 reported a simple, hassle-free, and in expensive method for the synthesis of nanoflower-shaped 3D copper oxide, wherein they utilized made use of the chemical bath deposition method which led to nanoflower-like copper oxide thin films. According to the surface morphological investigation, it is known that the adjoining nanoparticles are growing on a certain crystal orientation, which is due to the oriented arrangement and as a result forms nanoflowers of copper oxide.

Sekar et al. [52] in 2019 reported the synthesis of a copper oxide-based photocatalyst, which is prepared by a one-pot hydrothermal synthesis, and the nanostructure is known to show hierarchical morphology. The catalyst is known to degrade 4-chlorophenol and is used in hydrogen production reactions as well (Figure 10). Linfeng Gou et al. [53] in 2002 reported the facile synthesis of copper oxide nanocubes by using sodium ascorbate which is used to reduce Cu (II) salts when dissolved in water, and the reaction is said to happen in the presence of sodium hydroxide and surfactant. The resultant material thus

obtained is known to be a hollow structure. The team has also investigated the formation of the copper oxide nanocubes by substituting ascorbic acid in place of sodium ascorbate under lower concentrations of surfactant, and the particles so obtained are similar to those formed by the latter method. Chun Hong Kuo et al. [54] in 2008 reported a simple yet effective method of copper oxide synthesis by using copper salts reacting with surfactant, and a reducing agent. The resulting morphology of the obtained product is said to vary with the proportion of sodium dodecyl sulfate (SDS surfactant addition). The team was able to synthesize the morphological structures of copper oxide, such as truncated cubic, cuboctahedral, truncated octahedral, and octahedral shapes. The synthesized product was known to show good photocatalytic activity in degrading rhodamine B molecules efficiently (Figure 11). Lili Wan et al. [55] in 2019 reported the synthesis of Cu_2O by using a facile method to overcome the difficulty of copper oxide undergoing redox disproportionation reaction. In this, Cu_2O nanocubes are synthesized from bulk copper in the form of foam, and this synthesis methodology does not require the need of either surfactant or does not require pH control. By using techniques like sonication, a suspension was formed, centrifuged, and dried under a vacuum.

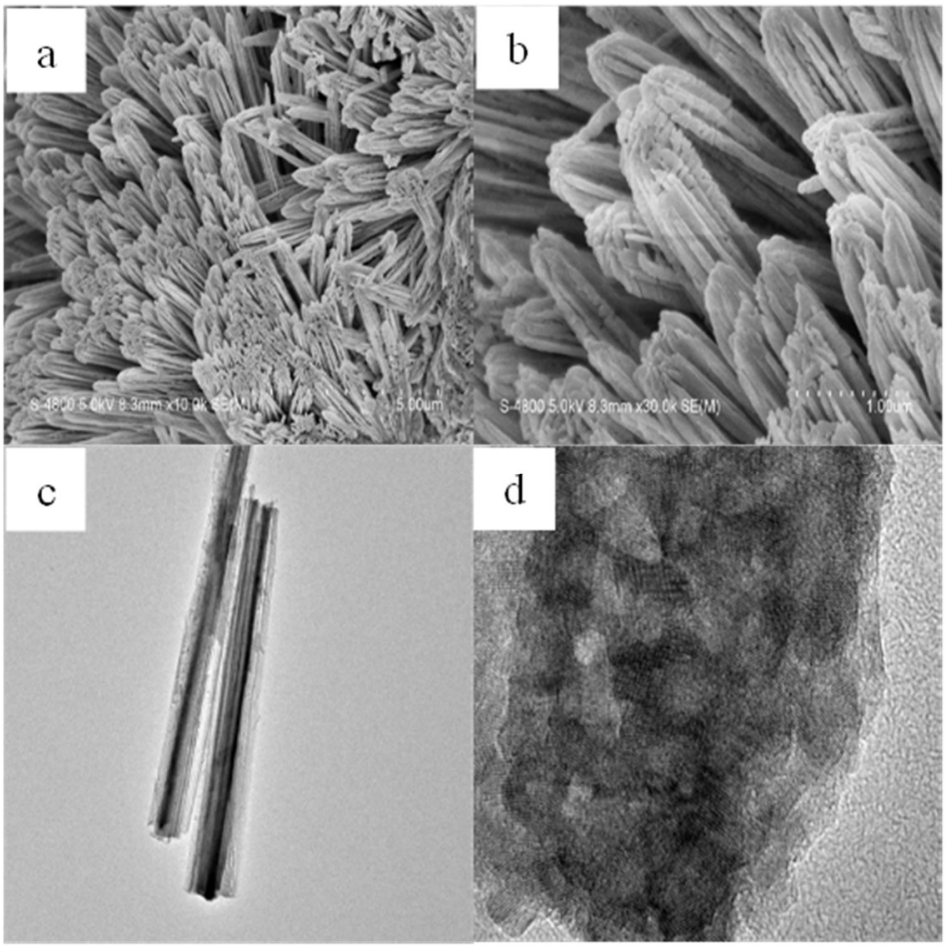

Figure 8. (**a**,**b**) Field emission scanning electron microscopy (FESEM) images oflow and high magnification of copper oxide (**c**,**d**) Typical high-resolution transmission electron microscopy (HRTEM) images of copper oxide nanostructure. Reproduced with permission from [49] Copyright The Royal Society, 2013.

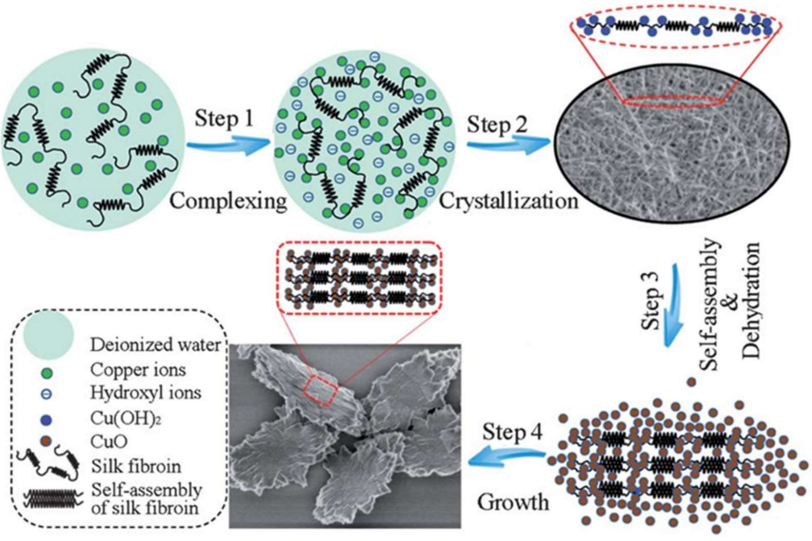

Figure 9. Possible formation mechanism of copper oxide almond-like nanoflower obtained after 48 h under reaction condition. Reproduced with permission from [50]. Copyright The Royal Society, 2013.

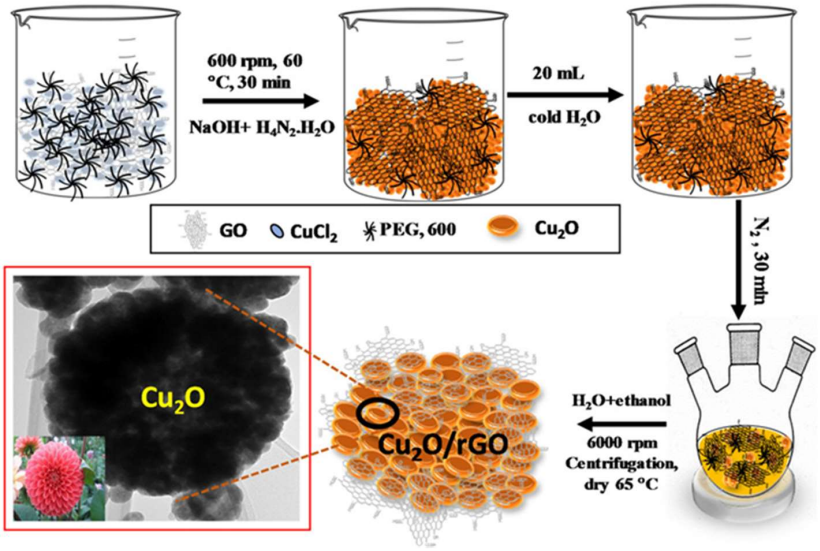

Figure 10. Schematic representation of the synthesis of Cu_2O/rGO nanocomposite photocatalyst. Reproduced with permission from [52]. Copyright Wiley-VCH Verlag GmbH& Co., 2020.

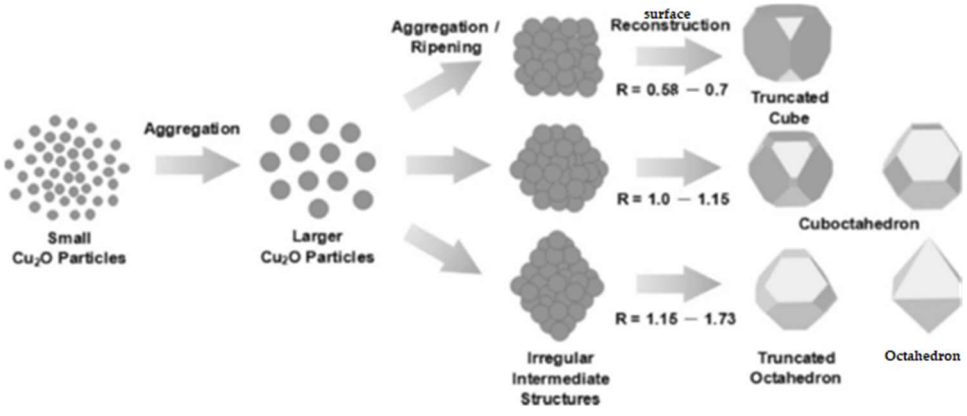

Figure 11. Pictoral representation of Cu_2O nanocrystal formation process. Reproduced with permission from [54]. Copyright American Chemical Society, 2008.

3. Photochemical Reduction of CO_2

The CO_2-reduction reaction utilizes the electrons and holes of the semiconductor available in conduction and valence band. The material should have the necessary band gap so as to minimize the charge recombination effects and restrict the redox cycling reactions. Despite the fact that both hydrogen evolution reaction (HER) and carbon dioxide-reduction reaction (CO_2RR) happening through photocatalysis were proven for the first time during a similar period, CO_2 reduction has received less attention than H_2 production. H_2 generation is a simple process which involves H^+ reduction. On the other hand, the mechanism of CO_2 reduction is more complicated, requiring CO_2 absorption, CO_2 activation, and product formation via a series of bond dissociations and bond formations with C–H, C–C stages on the catalysts surface [56]. The proton-assisted transfer of several electrons is widely accepted as the mechanism for CO_2 activation, whereas acceptance of a single e^- is a thermodynamically difficult process. Copper oxide-based materials have been used in a range of applications. Cuprous oxide (Cu_2O) are p-type semiconductors with 1.2 eV and 2.2 eV band gap energies, respectively. They can absorb a considerable part of solar light due to their narrow band gap. Because of narrowing and proper positioning of the valence and conduction bands, Cu_2O materials have been found to be excellent photocatalysts for CO_2 removal. In this work, we have keenly focused on the present-day progress in the branch of photocatalytic carbon dioxide reduction using cuprous oxide.

Ge Yin et al. [57] in 2015 reported the formation of carbon monoxide from carbon dioxide by using amorphous copper oxide as catalysts. By employing the wet chemical method, the top surface of the niobate (Nb_3O_8) nanosheets are grafted with nanoclusters of Cu (II). (Figure 12a) depicts a potential method for the process of photocatalysis which happens on the Cu (II) nanocluster-grafted niobate nanosheet. According to the electron spin resonance (ESR) analysis and isotopic labelling studies, the valence band possessing the excited holes of niobate nanosheets readily react with water molecules, and the conduction band bearing the excited electrons of Cu (II) nanoclusters inculcated with Nb_3O_8 nanosheets via the interface and are engaged in reducing the CO_2 moiety to CO. The carbon monoxide production is depicted in (Figure 12b). A 10% wt. of Cu (II) nanoclusters grafted niobate nanosheets yields 1.4 µmol of CO under UV irradiation.

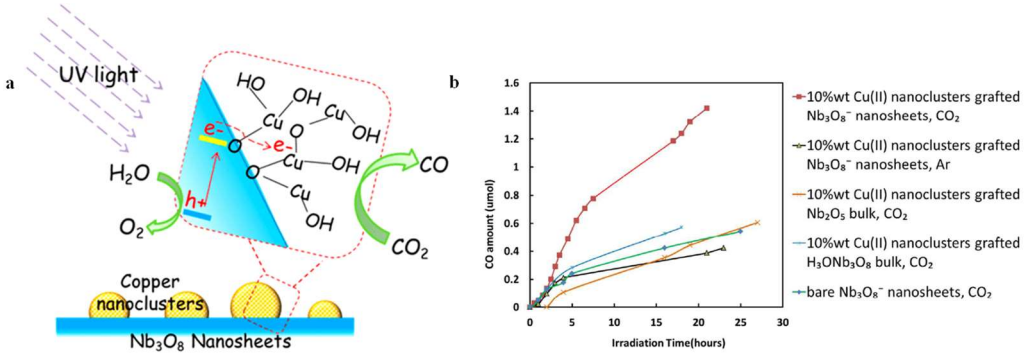

Figure 12. (**a**) Schematic representation of copper oxide nanocluster (**b**) carbon monoxide production of copper oxide nanocluster-grafted Nb_3O_8 nanosheets (UV irradiated) [57]. Copyright American Chemical Society, 2015.

Shahzad Ali et al. [16] in 2020 reported the reduced titania-Cu_2O heterostructure for the conversion to methane from CO_2 by photocatalysis. Synthesis involves the thermochemical reduction of TiO_2 and photodeposition of Cu_2O. The charge transfer mechanism, which prevents electron and hole recombination by achieving a spatial separation across the photocatalytic interface, confirmed the Z-scheme heterojunction and provided outstanding stability by suppressing Cu_2O photo corrosion. (Figure 13). The optimally reduced titania-Cu_2O sample produces a yield of 462 nmol/g of methane in 6 h and shows 42 h stability without using any co-catalysts.

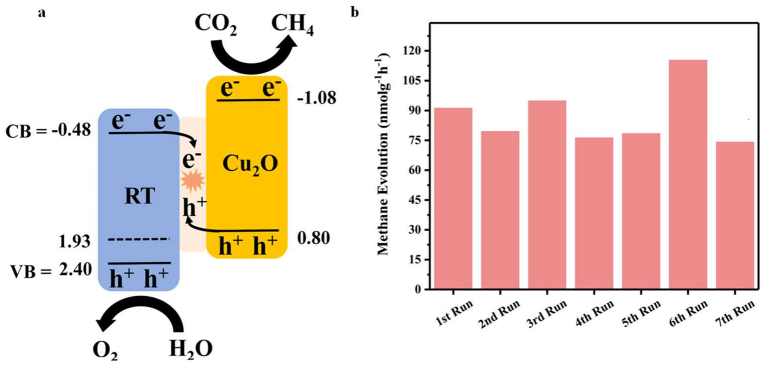

Figure 13. (**a**) Z-scheme charge transfer mechanism for reduced titania-Cu_2O heterostructure. (**b**) Methane production rate for seven sequential tests [16]. Copyright Elsevier B.V., 2020.

Xiaoqiang An et al. [58] in 2014 depicted the preparatory method of Cu_2O-reduced graphene oxide composite by the microwave-assisted chemical method for reducing CO_2 photocatalytically. The coupling of RGO with Cu_2O leads to the enhancement of activity by two times, which yields CO as the only reduction product. The increase in the yield is because of the retardation in the recombination of the electron hole pair, the protective nature of graphene oxide, and good charge transfer (Figure 14a,b). The XRD pattern of the pristine Cu_2O and composite are given in (Figure 14c). A noticeable quantum yield of 0.344% is obtained by using the visible radiations by employing Cu_2O/RGO junction for CO_2 reduction. Yield of CO by using different photocatalyst is depicted in (Figure 14d). The results emphasize the successful photocatalytic CO_2 reduction without using noble metal co-catalysts.

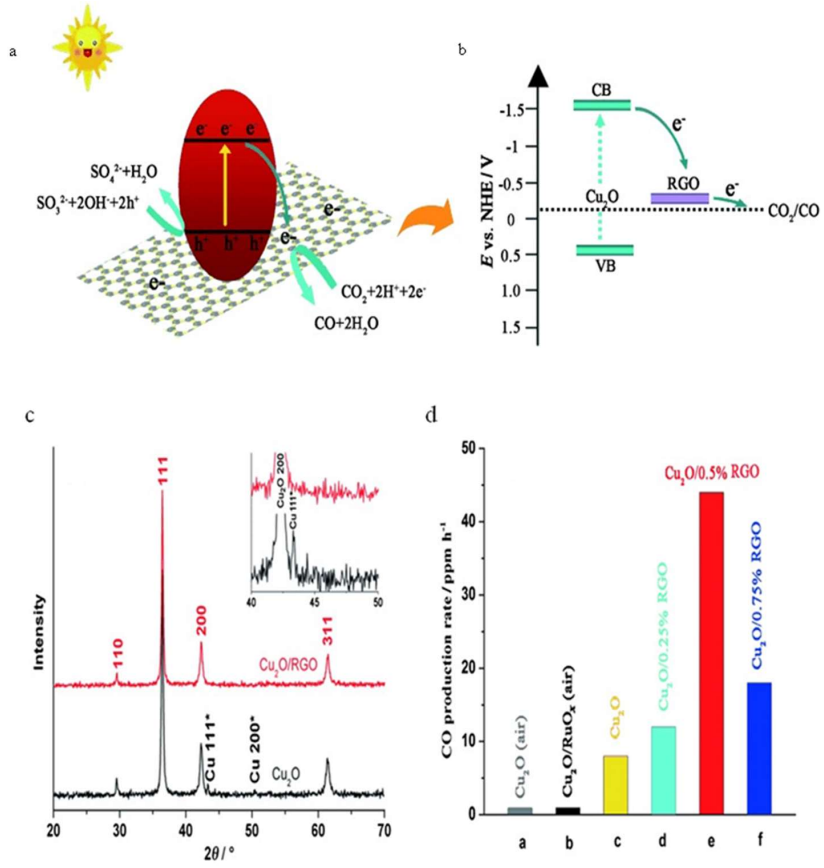

Figure 14. (**a**,**b**) Representation of the charge transfer mechanism in Cu_2O-RGO composites. (**c**) XRD data of Cu_2O and Cu_2O-RGO samples. (**d**) CO production rate using various catalysts [58]. Copyright Wiley-VCH Verlag GmbH& Co., 2014.

M.L Ovcharov et al. [59] in 2016 were able to carry out photocatalytic CO_2 reduction by using foam-structured Cu_2O. The results shows that the material has good photocatalytic ability for reducing CO_2 to aldehyde and methane. A previous report shows that a yield of 8.2 µmol/gcat/h and the latter gives a yield of 19.2 µmol/gcat/h (Figure 15). This change can be attributed to the expanded growth of copper oxide nanocrystals and the spatial arrangements of these crystals over the foam like 3D material. The yield of the as obtained aldehyde and methane under different wavelengths of light.

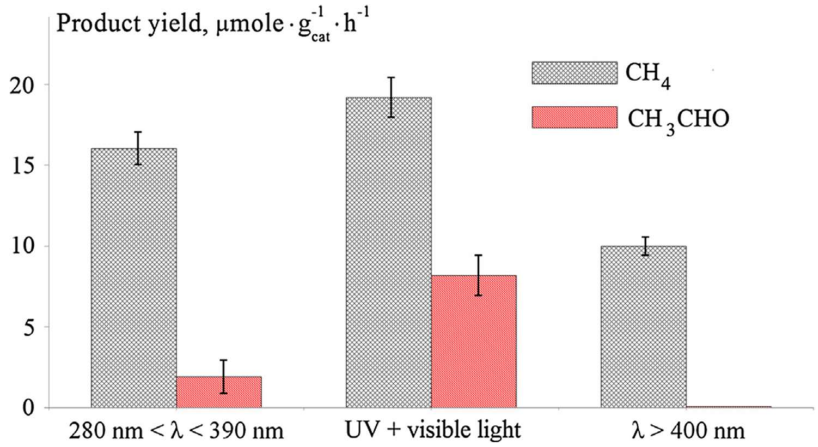

Figure 15. Product yield of form like Cu_2O catalyst under UV-visible radiations [59]. Copyright Elsevier B.V., 2016.

Ji Chao Wang et al. [60] in 2015 demonstrated the effective photoreduction of CO_2 activity over a direct Z-scheme α-Fe_2O_3/Cu_2O heterostructure under visible light irradiation. The facile hydrothermal deposition method is followed for the synthesis of Cu-Fe photocatalyst preparation, (Figure 16) via the reduction process. The Cu-Fe composites establish excellent photocatalytic performance in reducing CO_2 under visible light (>400 nm). The nominal amount of Cu_2O present in the obtained composite is known to be 50 mol%, and the CO crude yield obtained is 5.0 µmol/gcat upon irradiation for 3 h. The profound activity is attributed to the effective parting of the photoinduced electron hole pairs acquired from the constructed composite structure.

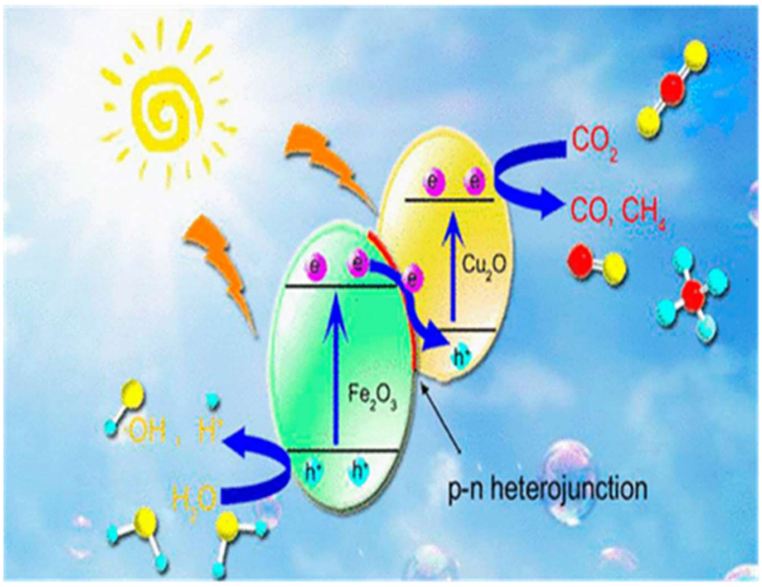

Figure 16. Schematic representation of charge transfer mechanism in Fe_2O_3-Cu_2O heterostructure [60]. Copyright American Chemical Society, 2015.

Chansol Kim et al. [61] in 2018 reported the synthesis of Z-scheme photocatalytic CO_2 conversion on 3D bismuth vanadate ($BiVO_4$) carbon-coated Cu_2O nanowire arrays by using visible light. The $BiVO_4$ and the copper oxide-coated carbon nanowires are found to have an uplifted light-harvesting property and charge separation ability, in 3D nanowires structure by the formation of a Z-scheme inducing charge flow. (Figure 17a). Apparently, CO formation rate of $BiVO_4$ carbon-coated Cu_2O was 9.4 and 4.7 times more effective than those of Cu_2O mesh and Cu_2O nanowires respectively (Figure 17b). The main reason for the improved activity is due to the enhancement of the light-harvesting ability and the surface area, which is mainly because of the 3D Cu_2O nanowires, and the activity increase is also attributed to the most feasible charge separation and transfer facilitated by the Z-scheme and the conductive carbon layer, and also due to the oxidation reduction potentials obtained with the Z-scheme.

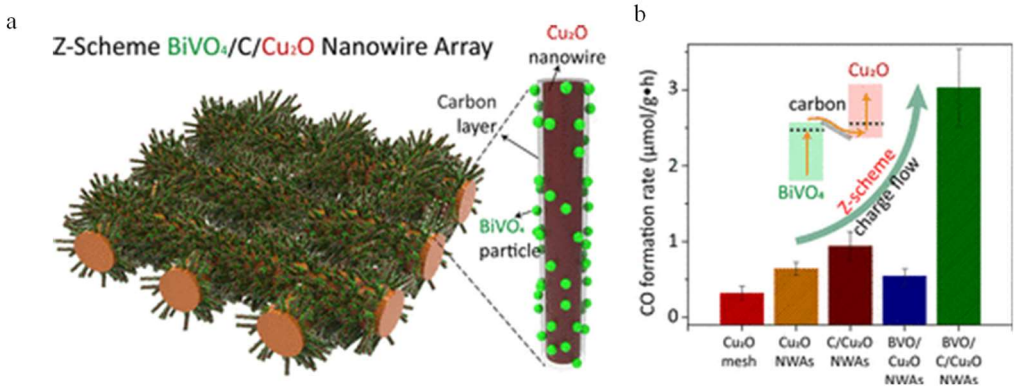

Figure 17. (**a**) Schematic representation of the synthesis of $BiVO_4$ carbon-coated Cu_2O nanowires. (**b**) Production rate of CO using different photocatalysts [61]. Copyright American Chemical Society, 2018.

Xiano Li et al. [62] in 2019 reported the development of Cu_2O-RGO-$BiVO_4$ nanocomposite using visible light for photocatalytic CO_2 reduction and benzyl alcohol oxidation. The Cu_2O-RGO-$BiVO_4$ nanocomposite was prepared through a thermal treatment of a Cu precursor in the presence of the pre-obtained RGO-$BiVO_4$. The spectroscopic studies shows that the surface of the RGO is known to have deposits of small nanoparticles of Cu_2O and olive-shaped $BiVO_4$. The formed Cu_2O-RGO-$BiVO_4$ nanocomposite displayed more photocatalytic activity, upon exposure to visible light, for the parallel process of reducing CO_2 and oxidation of benzyl alcohol, in comparison with bare a Cu_2O and RGO-$BiVO_4$ nanocomposite. The excellent photocatalytic ability observed over Cu_2O-RGO-$BiVO_4$ nanocomposite may be attributed to the presence of a Z-scheme charge transfer pathway, and the transfer of electrons that are photogenerated from $BiVO_4$ to Cu_2O in order to recombine through the RGO with the holes that are photogenerated, thus acting as a substitute for the virtuous electron transmitter. (Figure 18).

Po Ya Chang et al. [63] in 2018 have reported the cuprous oxide that had been embedded on the graphitic carbon nitride showed photocatalytic conversion of gaseous CO_2 via visible radiations. The combination of n-type g-CN and p-type Cu_2O crystals with an optimal surface composition and selecting Cu_2O crystals with enhanced photostability allowed CO_2 to be converted to CO. The cubic, all-corner-truncated rhombic dodecahedral and spherical morphology of Cu_2O is formed on g-CN (Figure 19a). The photocatalytic reduction of CO_2 is carried out by using Cu_2O and morphology-controlled Cu_2O-g-CN. The CO obtained is a major product from the main gaseous product in the reaction. It is observed that cubic Cu_2O-g-CN produces a maximum yield compared to other samples (Figure 19b). This is attributed to the dangling bonds on the surface of the dominant facet. The results show that the coupling of g-CN with Cu_2O crystals increased the reduction of CO_2 to CO by using visible light via the photocatalytic pathway.

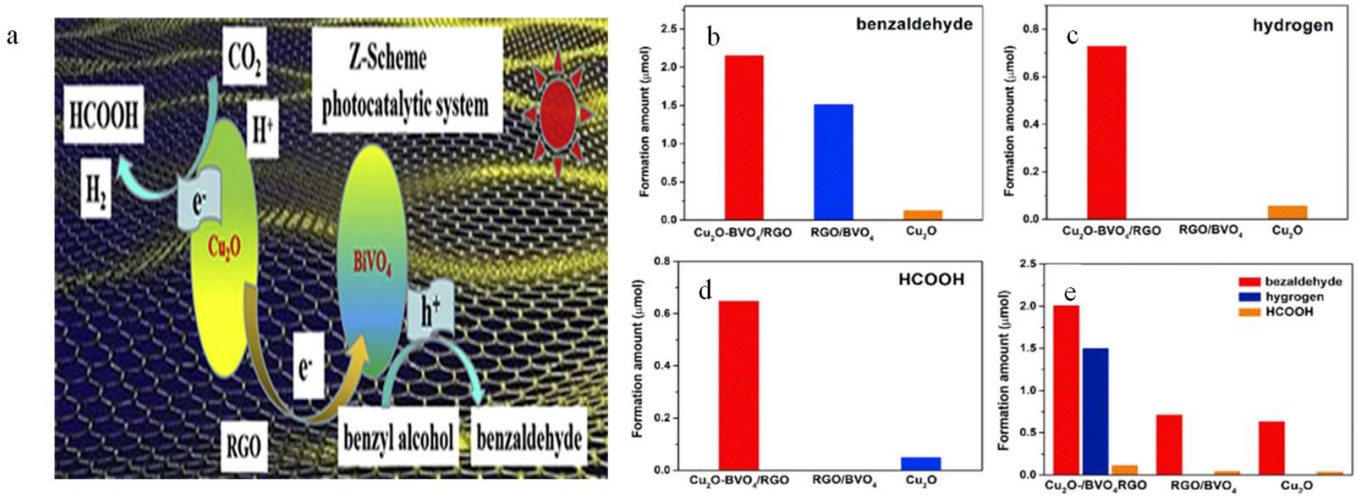

Figure 18. (**a**) Representation of the Z-scheme mechanism in the Cu_2O-RGO-$BiVO_4$ nanocomposite, CO_2 reduction using a different catalyst in the presence of benzyl alcohol. (**b**) Yield of benzaldehyde. (**c**) Yield of hydrogen. (**d**) Yield of formic acid (HCOOH). (**e**) Combined results [62]. Copyright Elsevier B.V., 2019.

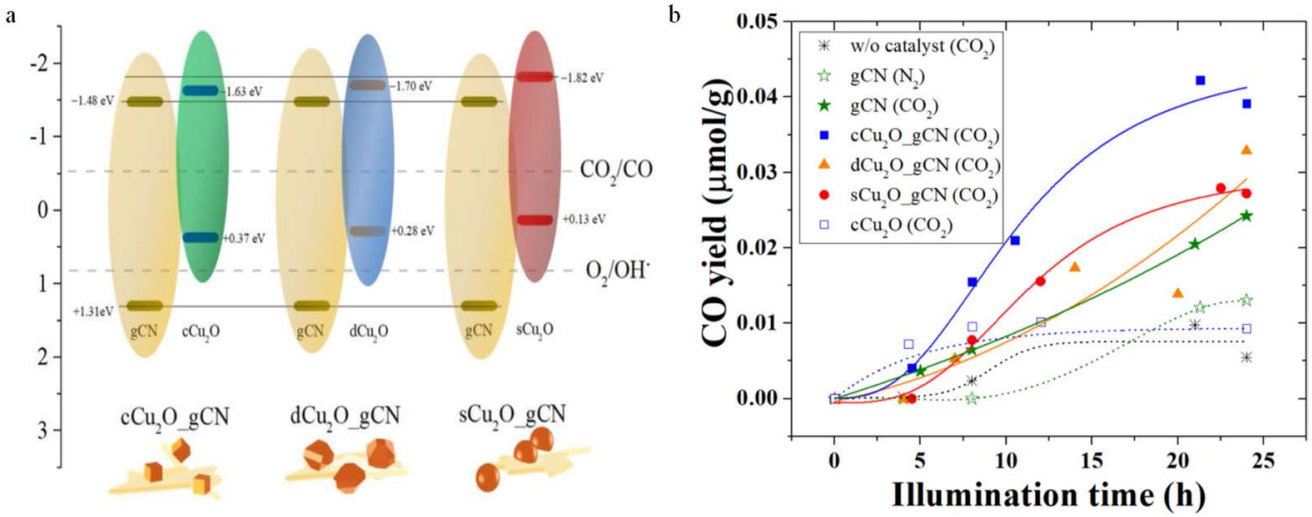

Figure 19. (**a**) Band structure of morphologically controlled Cu_2O. (**b**) CO production rate of various samples [63]. Copyright Elsevier B.V., 2018.

Matias E Aguirre et al. [64] in 2017 reported the synthesis of Cu_2O-TiO_2 composites for reduction of CO_2 via the Z-scheme mechanism. The composite of cuprous oxide molded with titanium oxide nanoparticles with high crystallinity and morphology are synthesized by using the solvothermal method. The spectroscopic studies reveal the p-n junction formation and type 2 alignment of the material. The reduction of CO_2 through photochemical pathway produces CO with production of 2.11 µmol/gcat/h, that is 4 times higher than for pure Cu_2O under similar parameters. The reaction is processed by using water vapor as a hole scavenger in UV-visible light radiations. The photocorrosion of cuprous oxide is shielded by titanium oxide and the Z-scheme mechanism acts as an effective way for the CO_2 reduction to take place in the composite (Figure 20).

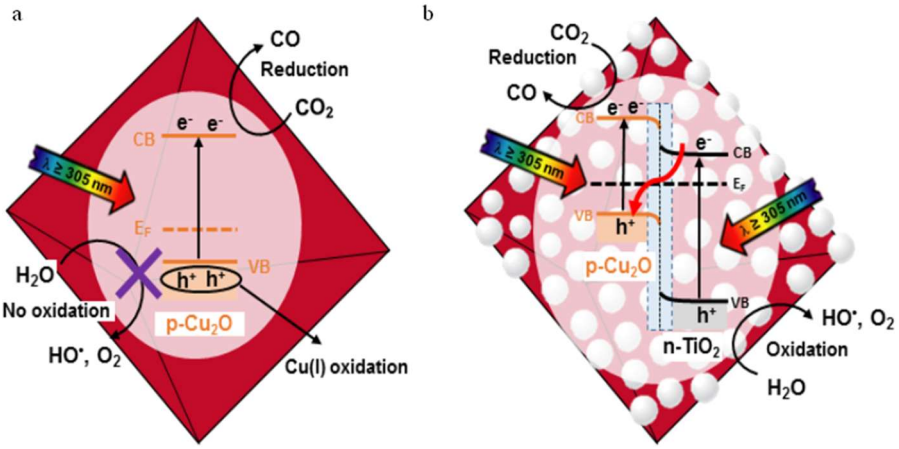

Figure 20. Representation of the charge transfer mechanism of CO_2 reduction under UV-visible light. (**a**) Octahedral Cu_2O. (**b**) Cu_2O-TiO_2 composite [64]. Copyright Elsevier B.V., 2017.

Fan Zhang et al. [65] 2020 reported the synthesis of Ag-Cu_2O-ZnO nanorods for CO_2 reduction by using the solvothermal method and the one-pot wet chemical reduction reaction. The 0.6Ag-0.4Cu_2O-ZnO composition produces 13.45 µmol/g CO, much higher than the reported production rate of pristine Cu_2O or ZnO. It has been observed that deposited Cu_2O can improve CO_2 chemisorption on catalyst surfaces, and that the developed Z-scheme charge transfer channel between ZnO and Cu_2O enables a highly effective charge separation, boosting catalyst photocatalytic activity (Figure 21a). The Ag nanoparticles act as a co-catalyst to further capture the surplus electrons deposited on Cu_2O's surface, alleviating Cu_2O's self-photoreduction and considerably improving the photocatalytic stability and activity of Ag-Cu_2O-ZnO nanorods (Figure 21b).

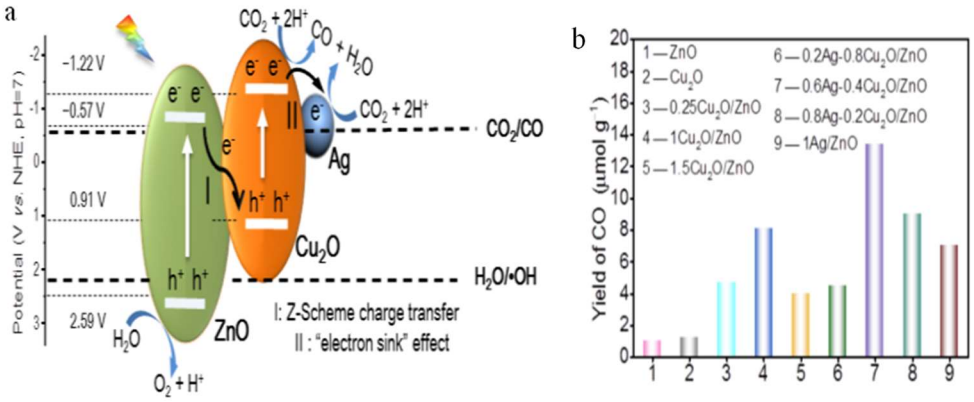

Figure 21. (**a**) Representation of the reaction mechanism for photocatalytic CO_2 reduction of the composite 0.6Ag-0.4Cu_2O-ZnO nanorods by using UV-visible light. (**b**) CO production using different materials [65]. Copyright Elsevier B.V., 2020.

Lili wan et al., [55] in 2019, elaborated the basis of surface chemistry, which states that there is efficient copper oxide photocatalysts, that has well defined nanocubical structure, that is employed in the synthesis of fuels by reducing carbon dioxide. They have stabilized the Cu_2O with the mixed oxidation state by driving in the gas phase of reduction of CO_2. The stabilized Cu_2O nanocubes have an ability to self-sustain by redox-active surface-frustrated lewis pairs (SFLP), which is evidence of effective photocatalysis (Figure 22).

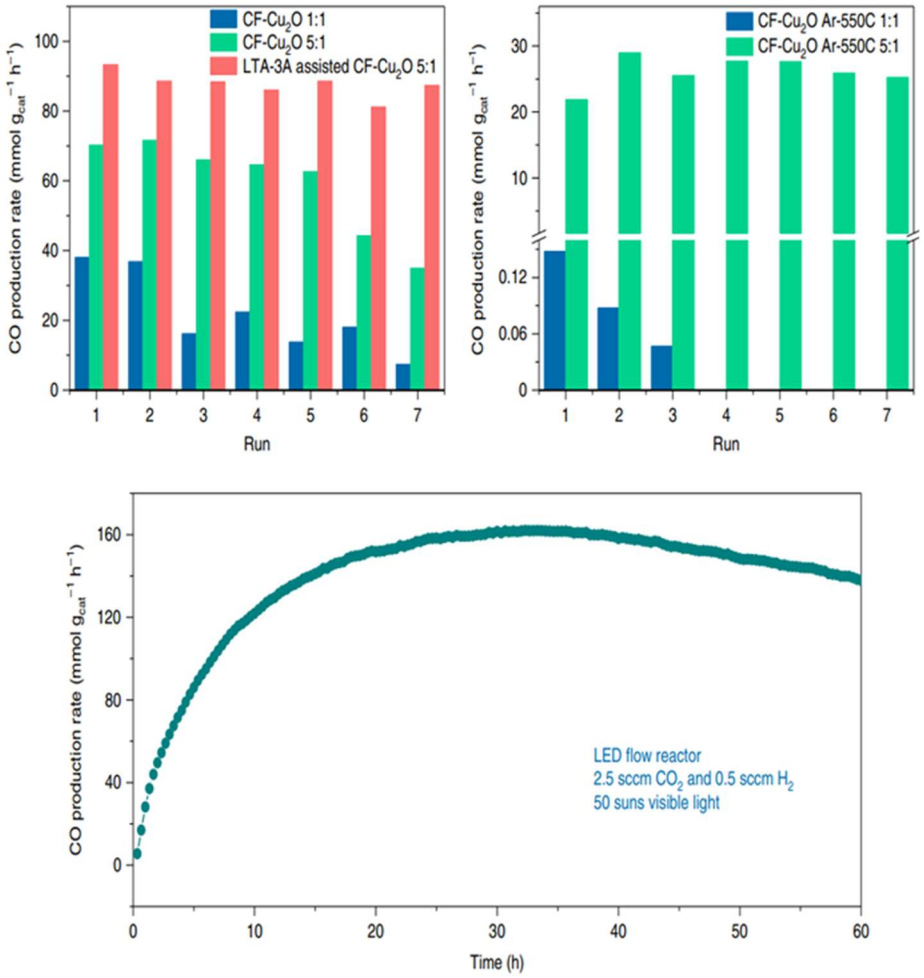

Figure 22. Photocatalytic activity of Cu_2O with overall CO_2 reduction [55]. Copyright Springer Nature, 2019.

Yimin a. Wu et al., [18] reported the synthesis of copper oxide which has facet specific active sites that aids in reducing carbon dioxide. Whilst the converting CO2 photocatalytically using liquid fuel methanol, with solar to fuel conversion having the major oxidation products of about 10% and the quantum yield was found to be approximately 72% (Figure 23).

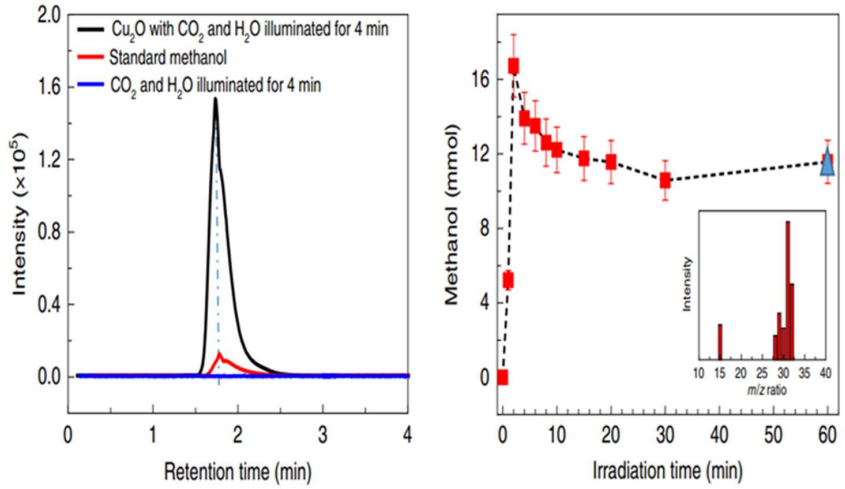

Figure 23. The carbon dioxide reduction to liquid fuel methanol (CH_3OH) [18]. Copyright Springer Nature, 2019.

4. Electrochemical Reduction of Carbon-Di-Oxide

The uplift of CO_2 utilization technologies like electrochemical CO_2 reduction (CO_2R) is urgently needed; as a result, this topic is being becoming a widespread area of interest in the field of research in the last few years. CO_2 reduction (CO_2R) by using renewable electrical energy has been advocated as a technique to reduce rising greenhouse gas emission [66]. Focusing on the electrochemical CO_2 reduction, the reaction taking place at the cathode, where the output is desirable for a sustainable environment by reducing the carbon footprint and thus accounting for cleaner fuel sources for energy of the future. Yoshio Hori and co-workers [67] published the first study in 1985 that quantified both liquid-phased and gaseous-phased products, accounting for 100%of Faradaic efficiency. The dimerization reaction of intermediate (* CO) must exceed a large potential barrier from the standpoint of reaction kinetics. However, prior to the dimerization step, *CO aims to desorb and liberate C_1 product, or sufficient adsorbed *H causes hydrogen evolution. The most popular electrochemical method for preparing metallic catalysts is electrodeposition. By applying voltage or current to a device containing three-electrode, the electrodeposition of the copper ions present in the electrolyte happens in the cathode substrate. The electrode surface can be recreated in an electrochemical environment by modifying the electrochemical conditions or modifying the electrolyte composition. The electrochemical carbon dioxide reduction reaction (CO_2RR) is a promising possibility for turning electricity into permanent forms of chemical energy for long-term storage of renewable energy [68]. There are reports of CO_2 being selectively converted to CO by using a low-cost electrocatalyst consisting of tin nanoparticles on copper oxide nanowires. The electrode is prepared via electroless deposition, a straightforward and cost-efficient surface alteration process. At low overpotentials, hybrid electrode demonstrates outstanding selectivity, activity, and durability [69]. In aqueous solutions, by transferring electrons and protons electrocatalytically, CO_2-reduction products are carbon-containing compounds such as methane (CH_4), carbon monoxide (CO), methanol (CH_3OH), formic acid (HCOOH), ethanol (C_2H_3OH), and ethylene (C_2H_4) [70].

CO_2 reduction in copper catalysts allow C^{2+} products to evolve which is peculiar. Product distribution varies greatly depending on the catalyst's synthesis: in oxide-based copper, nanoparticles yield ethylene and ethanol whereas nanoparticles derived from copper generate primarily methane and hydrogen (Figure 24) [71].

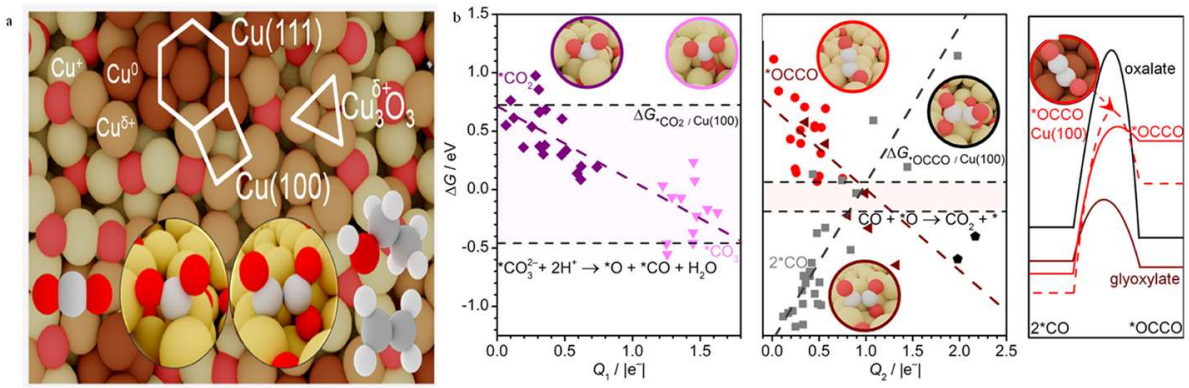

Figure 24. (**a**) Graphic representation of 0D-Cu CO_2R activity and (**b**) its catalytic activity with response to the electrocatalytic activity [71]. Copyright American Chemical Society, 2020.

Using 0D copper oxide-based electrodes as electrocatalysts, the efficiency and selectivity both improved favorably for CO_2 reduction. This is due to the fact that many low coordination sites, rich-grain boundaries and a specific number of oxygen species are common features. All of these are thought to improve C^{2+} production with better selectivity and catalytic activity. Quite critically, it is thought that surface Cu^+ plays a vital role. A Cu^+ site has greater stability than a metallic Cu^0 region for CO, in particular. The dimerization

process on the 0D-Cu catalysts is favorable for increased production of C^{2+} products in both kinetic and thermodynamic strategies [72].

Cu is indeed the exclusive metal that aids in electrochemically converting CO_2 into usable fuels and chemicals, so there seems to be an extensive investigation of copper (Cu) nanomaterials in these reactions. Cu is one of the superior catalyst that demonstrates electrochemical CO_2 reduction (CO_2R) and has a proclivity for producing value-added hydrocarbon products such as ethylene and ethanol [73].

Jiang et al. [74] in 2018 anodically oxidized copper foil to make Cu $(OH)_2$ nanowires (AN-Cu) by continuous current anodic oxidation on the copper foil. Cu^{2+} was abundant on the catalyst surface; however, species with low valence such as Cu^+ and Cu^0 were clearly observed by reduction of Cu^{2+} with the course of the reaction (Figure 25). Copper with a mixed valence could be linked to ethylene synthesis intermediates. Furthermore, the catalysts' compositions, surface structure, and catalytic activity were all altered.

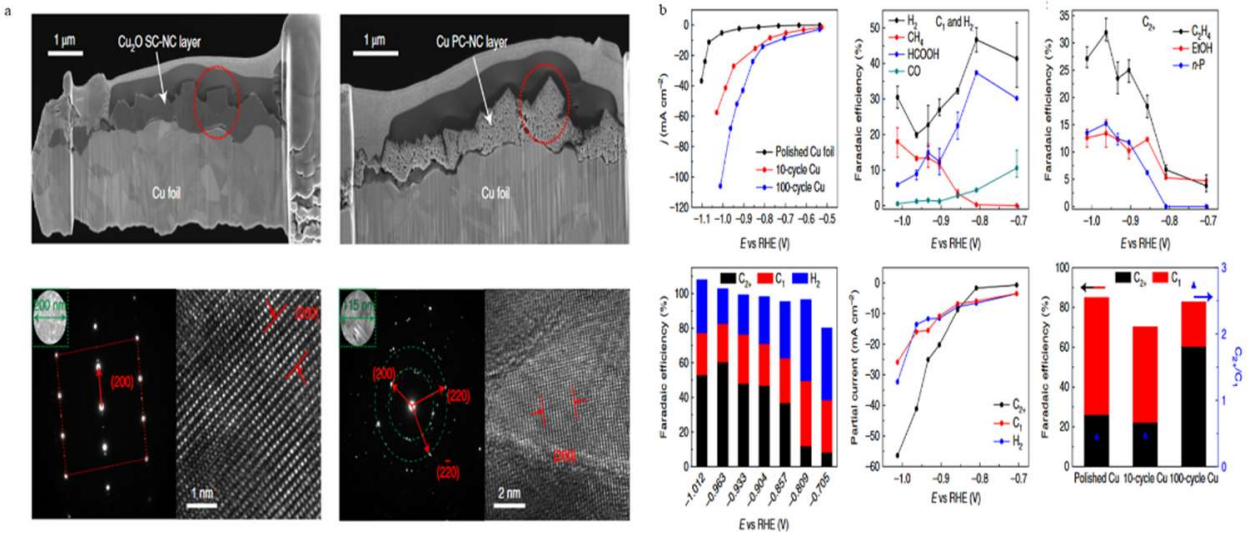

Figure 25. (**a**) Morphological studies of the synthesized Cu_2O and (**b**) the electrocatalytic activities of CO_2 reduction [74]. Copyright Springer Nature, 2018.

Hyejin Jung. et al. [75] in 2019 elaborated that during the initial CO_2RR, the synthesized nanospringe particle catalyst showed increased activity, and Faradaic efficiency is tripled to 57.3% from 27% in ethylene (C_2H_4) generation. The morphological modification throughout the reaction time was linked to increasing C_2H_4 production activity. Under the negative potential, 2–4 nm tiny particles were fragmented from the 20-nm cubic Cu_2O crystalline particles and the fragmentation was observed to start from the nanocrystal's surface. (Figure 26).

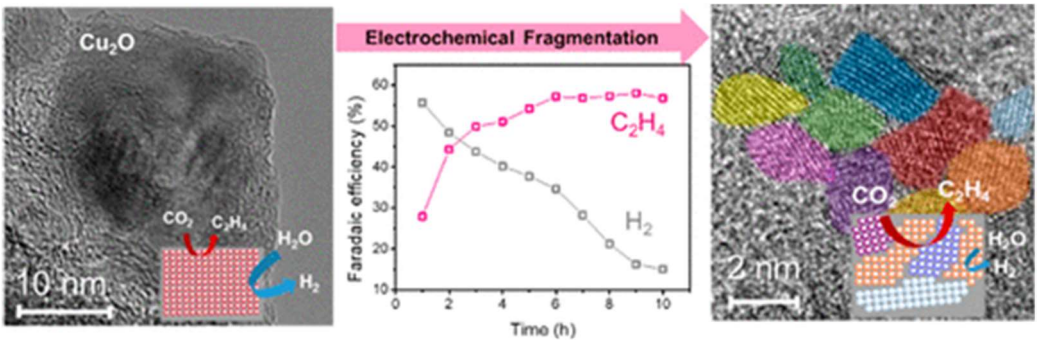

Figure 26. CO_2RR performance representing from morphological and electrochemical studies of fragmented copper-based nanoparticle/C [75]. Copyright American Chemical Society, 2019.

Lily Mandal et al. [76] in 2018 explored carbon dioxide reduction with Cu_2O nanoneedles, Cu_2O nanocrystals, and Cu_2O nanoparticles. The authors utilized in situ Raman spectroscopy, computational modelling, and selected-ion flow tube mass spectrometry in conjunction with chronopotentiometry. The metallic copper was attained by the surface of copper oxide reduction in selective production of gaseous C^2 products (i.e., C_2H_4) in CO_2R (Figure 27). Until the reduction of Cu_2O into Cu_2OR on the surface completely, no CO_2R products are formed, as it is kinetically and energetically more advantageous than CO_2R, according to density functional theory.

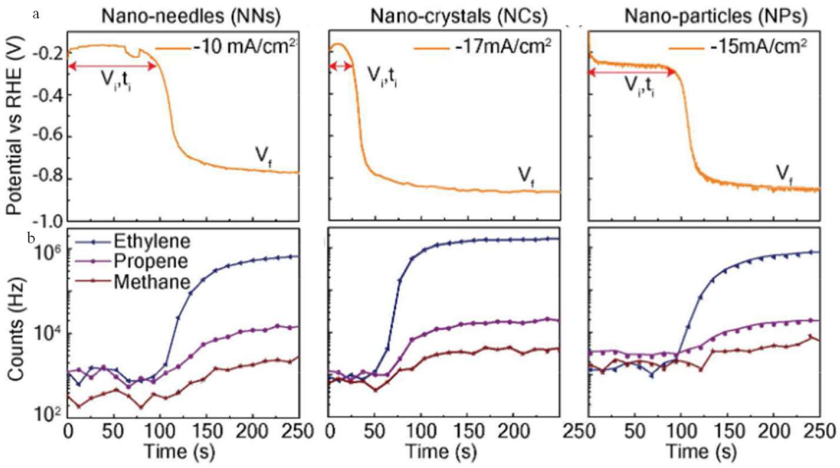

Figure 27. At low current density evolution of CO and H_2. (**a**) In chronopotentiometry analysis for the nanoneedles, nanocrystals, and nanoparticles with electrolyte as 0.1 M $KHCO_3$ which is essentially saturated with 1 atm CO_2, and (**b**) GC plot with current application, in electrolyte of 0.1 M $KHCO_3$ [76]. Copyright American Chemical Society, 2018.

Animesh Roy, et al. [77] in 2021 reported the controlled and direct production of Cu_2O, which was made into a composite thin film on conductive nickel foam by using the electrodeposition technique for CO_2 to CH_3OH (i.e., carbon dioxide to methanol conversion electrochemically). At room temperature, the electrocatalytic reduction was carried out in a CO_2-saturated aqueous solution including $KHCO_3$, pyridine, and HCl. The electrochemical performance of the produced electrocatalysts at a potential of 1.3 V takes place for 2 h for CO_2 reduction. The Cu_2O composite has a current density of 46 mA/cm^2 for (Figure 28), indicating superior electrocatalytic activity. The developed catalyst has a potential to be a highly efficient and selective electrode for methanol synthesis.

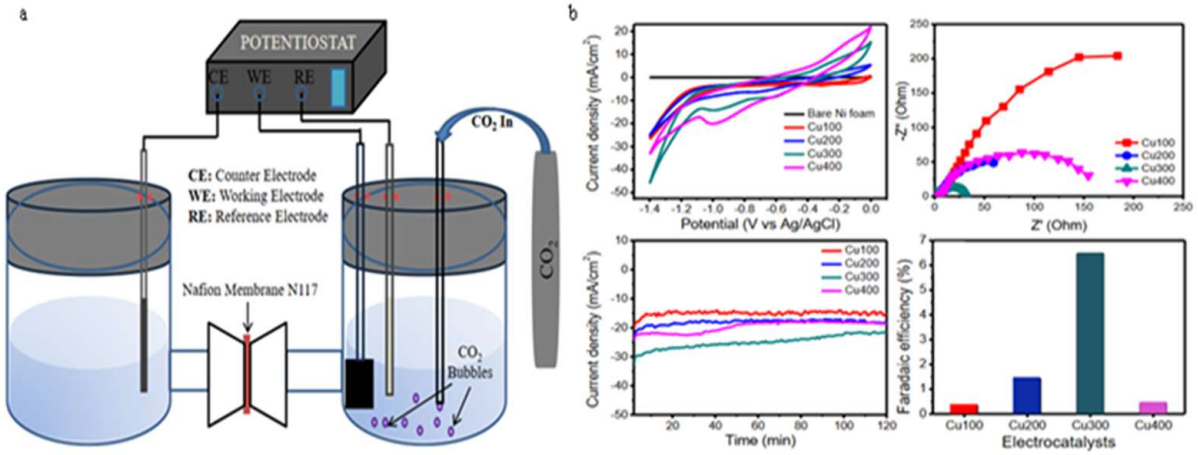

Figure 28. (**a**)The graphical representation of the electrochemical setup connected via nafion membrane and (**b**) its electrocatalytic activity [77]. Copyright Elsevier B.V., 2021.

Mengran Li et al. [78] in 2020 explained the time for electrodeposition of tin on copper oxide-derived substrate with relationship to the selectivity of carbon dioxide reduction to formate. The formate Faradaic efficiency was about 81% at 1.1 V vs. a reversible hydrogen electrode (RHE), along with the electrodeposition of tin, which is 37% greater than tin foil and sample for a time interval of 684 s (Figure 29).

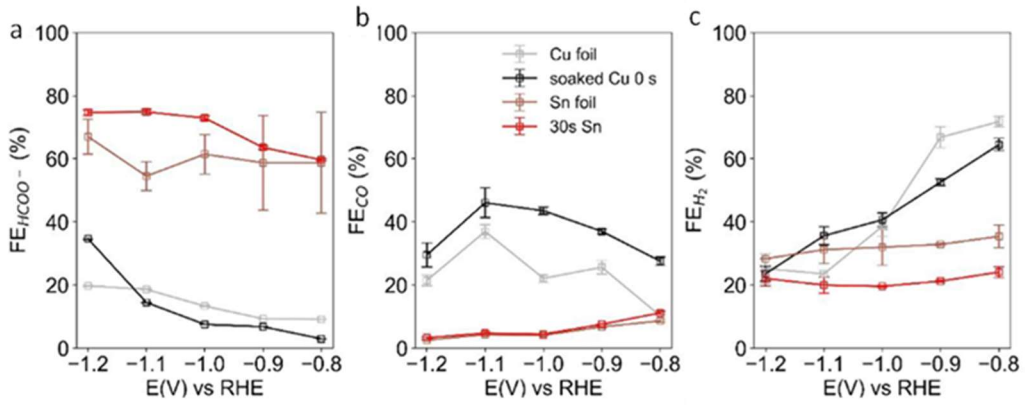

Figure 29. The Faradaic efficiency (FE) comparison (**a**) formate, (**b**) CO, and (**c**) H_2 in 0.5M $KHCO_3$ electrolyte which is saturated in CO_2 [78]. Copyright American Chemical Society, 2020.

Chao Zhan et al. [79], in 2021 elaborated on the Faradaic efficiency in CO_2RR in multicarbon compounds which has similarity with Cu–CO stretching band to CO rotation band and has a volcanic pattern intensity ratio (Figure 30). By operando Raman spectroscopy, the percentage efficiency of the formation of ethylene, ethanol (EtOH), and 1-propanol (PrOH) and the sum of all C^{2+} products, and H_2 and CO were recorded during an electrocatalytic reaction.

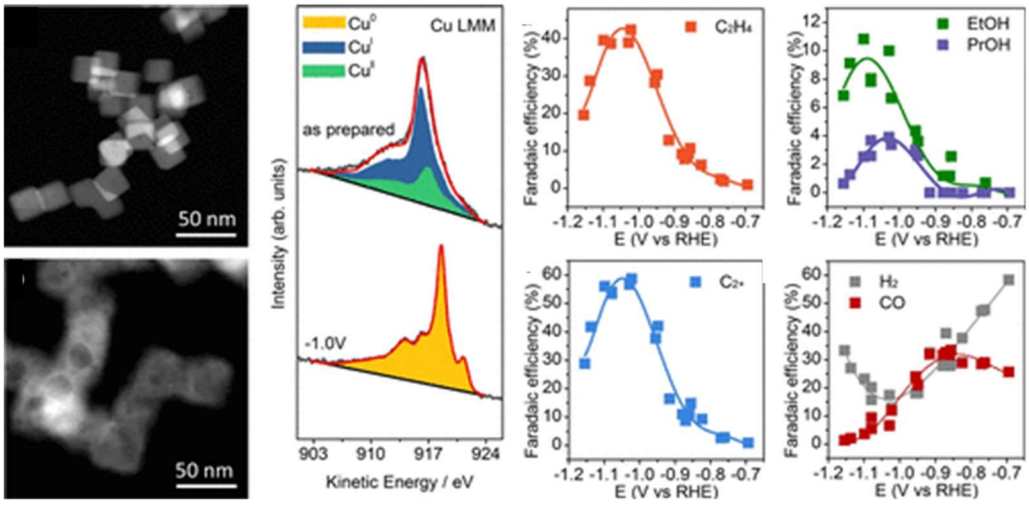

Figure 30. Upon 1 h of CO_2RR, potential-dependent F.E. of ethylene, ethanol (EtOH), and 1-propanol (PrOH), the sum of all C^{2+} products, and H_2 and CO [79]. Copyright American Chemical Society, 2021.

Christina W. Li et al. [80], in 2012 reported Cu electrodes of copper were modified by placing Cu under heat treatment in the presence of air and decreasing the oxide formed by using electrochemical method. The thickness of the layered copper oxide highly influences the effectiveness of the electrodes. The polycrystalline copper electrodes and Cu_2O electrodes with layered structure produced by heating at 130 °C confirmed similar activity. At overpotentials of 0.4 V, the blending of these properties resulted in CO_2 reduction with more efficiency than other reported works under similar parameters (Figure 31). However, the efficiency of the modified material remained steady for many hours, but the copper with polycrystalline structure became inactive within 1 h. The electrodes shown here are

valuable in explaining the structural characteristics of Cu that regulate the reduction of H_2O and CO_2, as well as a capable electrocatalyst. Hence, through complete utilization of Cu_2O as an efficient electrocatalyst can pave the way to the higher Faradaic efficiency along with the choice of a supporting composite material can make the Cu_2O economically sustainable and eco-friendly for CO_2 reduction.

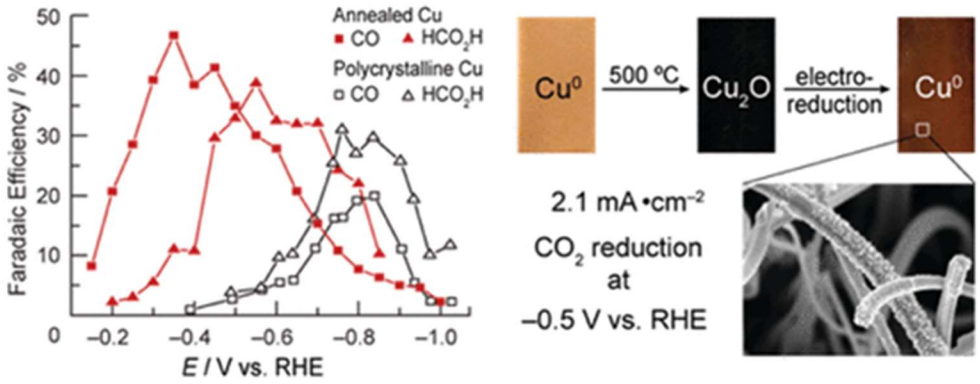

Figure 31. The overall representation of electrocatalytic activity of Cu_2O [80]. Copyright American Chemical Society, 2012.

Chunliu Yan et al., in 2022 [81] reported the N-doped Cu_2O showed good modes of intermediates and selectivity and productivity in electroreduction of CO_2 and the composite resulted in a two-fold increase in production of CO and C_2H_4 than bare Cu_2O (Figure 32).

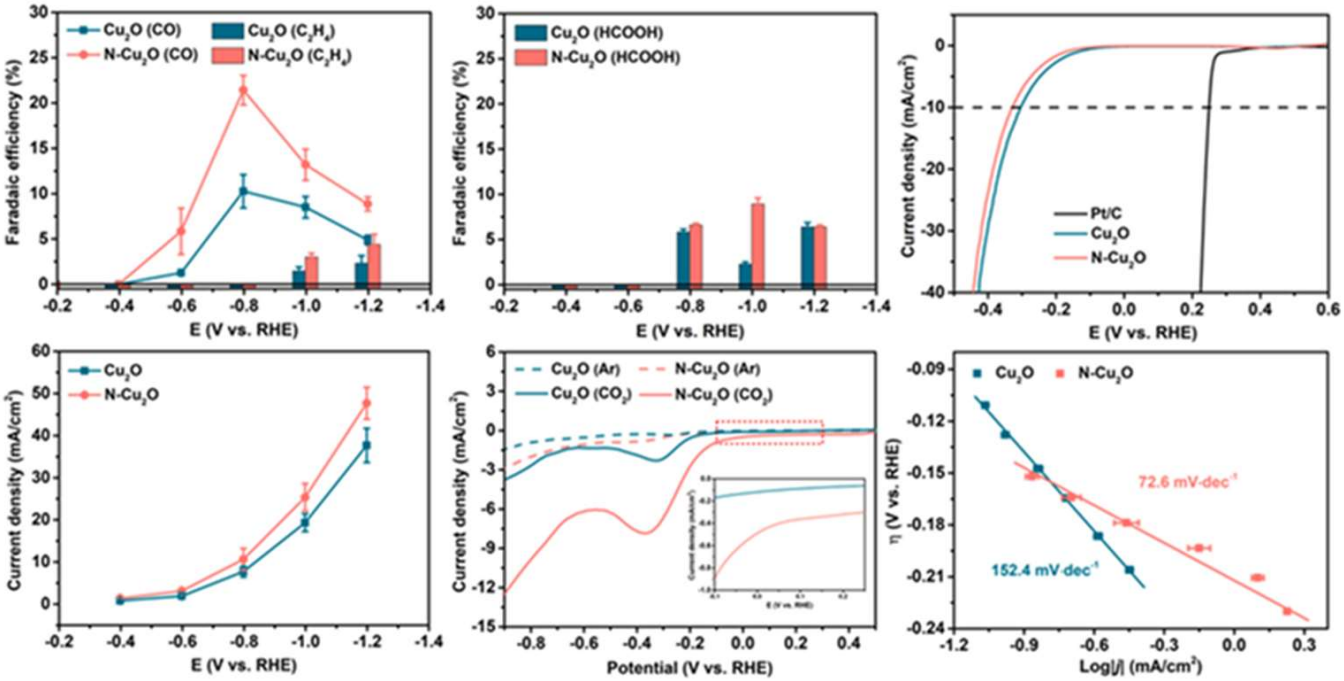

Figure 32. The overall representation of electrocatalytic activity of Cu_2O [81]. Copyright Elsevier B.V., 2022.

Jinze Liu et al., in 2021 [82] reported the stability of Cu2O in the negative potential in reducing the CO_2 for production of C_2. The authors have highlighted stable Cu_2O and fact finding for increased Faradaic efficiency of 73%, which is 1.5 times higher than other available Cu_2O, which might be due to the Cu^+ species promoting the C-C coupling (Figure 33).

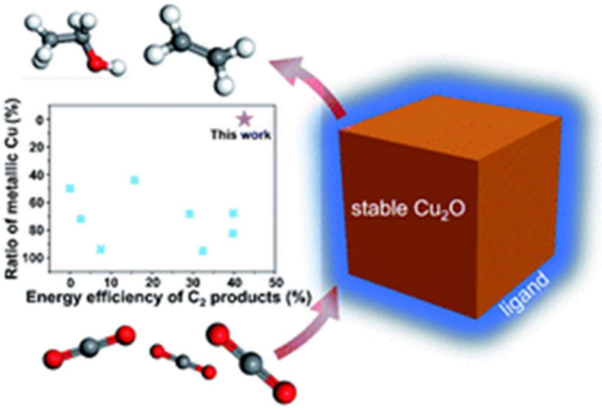

Figure 33. The overall graphic representation of CO_2 reduction [82]. Copyright The Royal Society, 2022.

Haiqiang Luo et al., in 2022 [83] outreached the reduction of CO_2 to ethylene and syngas by surface modification of nano-Cu_2O and methodically explored the rule of facet dependence. The authors contributed a novel method to improve the product selectivity for ethylene generation (74.1%) in neutral electrolyte (Figure 34).

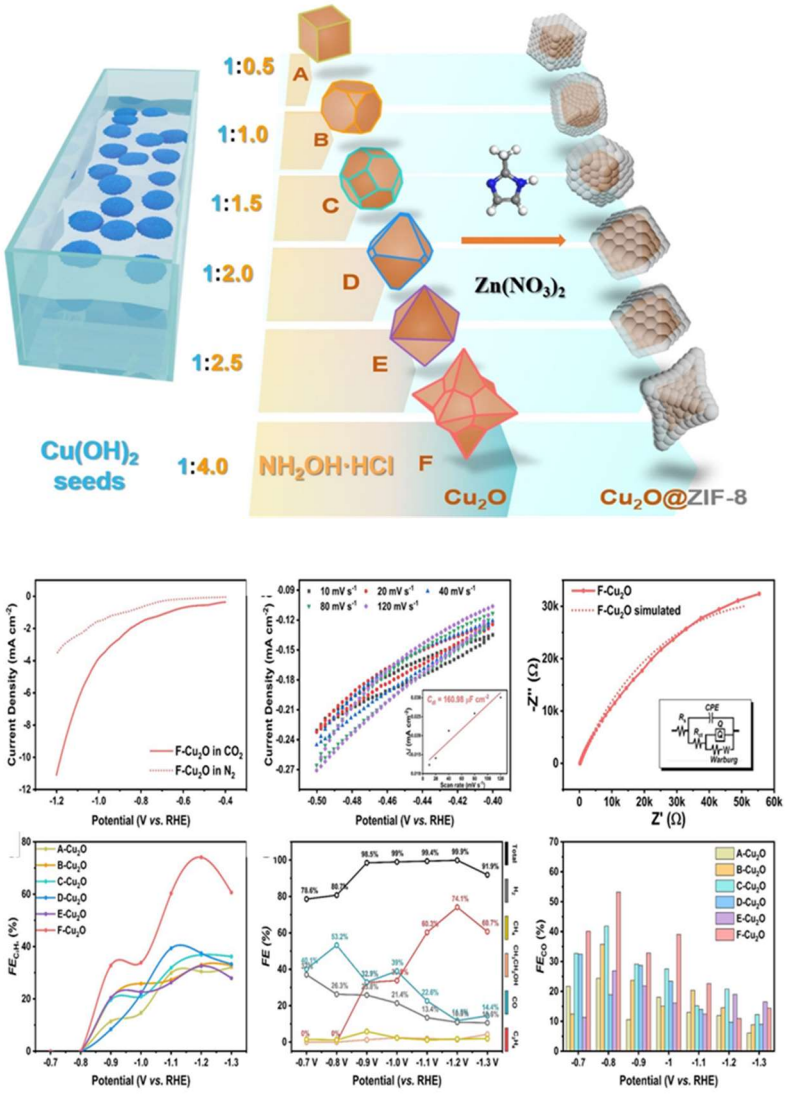

Figure 34. The systematic synthesis with changes in morphology and overall electrocatalytic activity of CO_2 reduction [83]. Copyright John Wiley & Son, 2022.

To conclude, the efficient utilization of Cu_2O as an efficient electrocatalyst can pave the way to the higher Faradaic efficiency, further preparing Cu_2O-supporting composite material that may provide opportunities to recover and reuse the catalyst, and thus make the catalyst environmentally sustainable and economically feasible for CO_2 reduction.

5. Conclusions

This review is the comprehensive study of copper oxide synthesis and its application towards CO_2 reduction via photochemical and electrochemical methods. The synthesis of Cu_2O in various dimensions from 0D to 3D is described extensively. This article outlines recent developments and breakthroughs in the electrochemical or photochemical conversion of CO_2 to usable chemical fuels. Even though electrocatalytic and photocatalytic CO_2 reduction have made tremendous progress in recent decades, they are burgeoning fields of study, due to their uncontrolled reaction activity and selectivity. To compete with alternative fuel production technologies, there is currently no rigorous techno-economic method established to promote the goal of reducing production costs of chemical fuels from CO_2 reduction. CO_2 reduction is important from a theoretical as well as a practical standpoint. Despite significant obstacles, there is no reason to deny its enormous potential and influence to make CO_2 reduction a viable solution for a carbon-neutral future. More effort is needed in fundamental knowledge, materials research, and catalyst engineering.

Author Contributions: S.M., data curation, conceptualization, methodology, resources, methodology; B.H., data curation, conceptualization, methodology, resources, methodology; A.A., data curation, conceptualization, methodology, resources, methodology; M.S., data curation, conceptualization, methodology, resources, methodology; C.C., conceptualization, validation, visualization; K.S. (Keiko Sasaki), conceptualization, supervision, validation, visualization; B.R., conceptualization, methodology, supervision, validation, visualization; K.S. (Karthikeyan Sekar), conceptualization, investigation, methodology, supervision, validation, visualization. All authors have read and agreed to the published version of the manuscript.

Funding: This research received no external funding.

Institutional Review Board Statement: Not applicable.

Informed Consent Statement: Not applicable.

Data Availability Statement: No data availability statement.

Acknowledgments: S.K. acknowledges the Royal Society-Newton International Fellowship Alumni follow-on funding support AL\211016, UK and Department of Chemistry at the SRM Institute of Science and Technology, India. We thank SRM-IST for the PhD student fellowship. BR thank the Director, CSIR-IMMT for the encouragement and support.

Conflicts of Interest: The authors declare no conflict of interest.

References

1. Available online: https://www.climate.gov/news-features/understanding-climate/climate-change-atmospheric-carbon-dioxide (accessed on 3 March 2022).
2. Ye, W.; Guo, X.; Ma, T. A review on electrochemical synthesized copper-based catalysts for electrochemical reduction of CO_2 to C2+ products. *Chem. Eng. J.* **2021**, *414*, 128825. [CrossRef]
3. Available online: https://wedocs.unep.org/bitstream/handle/20.500.11822/30797/EGR2019.pdf (accessed on 4 March 2022).
4. Available online: https://www.eia.gov/outlooks/ieo/ (accessed on 3 March 2022).
5. Hu, B.; Guild, C.; Suib, S.L. Thermal, electrochemical, and photochemical conversion of CO_2 to fuels and value-added products. *J. CO2 Util.* **2013**, *1*, 18–27. [CrossRef]
6. Zhu, X.; Li, Y. Review of two-dimensional materials for electrochemical CO_2 reduction from a theoretical perspective. *WIREs Comput. Mol. Sci.* **2019**, *9*, e1416. [CrossRef]
7. Li, K.; Peng, B.; Peng, T. Recent Advances in Heterogeneous Photocatalytic CO_2 Conversion to Solar Fuels. *ACS Catal.* **2016**, *6*, 7485–7527. [CrossRef]
8. Xu, S.; Carter, E.A. Theoretical Insights into Heterogeneous (Photo)electrochemical CO_2 Reduction. *Chem. Rev.* **2018**, *119*, 6631–6669. [CrossRef]

9. Yu, S.; Yang, N.; Liu, S.; Jiang, X. Electrochemical and photochemical CO_2 reduction using diamond. *Carbon* **2021**, *175*, 440–453. [CrossRef]
10. Wu, J.; Huang, Y.; Ye, W.; Li, Y. CO_2 Reduction: From the Electrochemical to Photochemical Approach. *Adv. Sci.* **2017**, *4*, 1700194. [CrossRef]
11. Hori, Y.; Murata, A.; Kikuchi, K.; Suzuki, S. Electrochemical reduction of carbon dioxides to carbon monoxide at a gold electrode in aqueous potassium hydrogen carbonate. *J. Chem. Soc. Chem. Commun.* **1987**, *1987*, 728–729. [CrossRef]
12. Watanabe, M.; Shibata, M.; Kato, A.; Azuma, M.; Sakata, T. Design of Alloy Electrocatalysts for CO_2 Reduction: III. The Selective and Reversible Reduction of on Cu Alloy Electrodes. *J. Electrochem. Soc.* **1991**, *138*, 3382–3389. [CrossRef]
13. He, J.; Johnson, N.J.J.; Huang, A.; Berlinguette, C.P. Electrocatalytic Alloys for CO_2 Reduction. *ChemSusChem* **2018**, *11*, 48–57. [CrossRef]
14. Zheng, Y.; Duan, Z.; Liang, R.; Lv, R.; Wang, C.; Zhang, Z.; Wan, S.; Wang, S.; Xiong, H.; Ngaw, C.; et al. Shape-dependent performance of Cu/Cu_2O for photocatalytic reduction of CO_2. *ChemSusChem* **2022**. [CrossRef] [PubMed]
15. Zhang, Y.; Pan, D.; Tao, Y.; Shang, H.; Zhang, D.; Li, G.; Li, H. Photoelectrocatalytic Reduction of CO_2 to Syngas via SnOx-Enhanced Cu_2O Nanowires Photocathodes. *Adv. Funct. Mater.* **2022**, *32*, 2109600. [CrossRef]
16. Ali, S.; Lee, J.; Kim, H.; Hwang, Y.; Razzaq, A.; Jung, J.W.; Cho, C.H.; In, S.I. Sustained, photocatalytic CO_2 reduction to CH4 in a continuous flow reactor by earth-abundant materials: Reduced titania-Cu_2O Z-scheme heterostructures. *Appl. Catal. B Environ.* **2020**, *279*, 119344. [CrossRef]
17. Call, A.; Cibian, M.; Yamamoto, K.; Nakazono, T.; Yamauchi, K.; Sakai, K. Highly Efficient and Selective Photocatalytic CO_2 Reduction to CO in Water by a Cobalt Porphyrin Molecular Catalyst. *ACS Catal.* **2019**, *9*, 4867–4874. [CrossRef]
18. Wu, Y.A.; McNulty, I.; Liu, C.; Lau, K.C.; Liu, Q.; Paulikas, A.P.; Sun, C.J.; Cai, Z.; Guest, J.R.; Ren, Y.; et al. Facet-dependent active sites of a single Cu_2O particle photocatalyst for CO_2 reduction to methanol. *Nat. Energy* **2019**, *4*, 957–968. [CrossRef]
19. Xiong, Z.; Lei, Z.; Kuang, C.C.; Chen, X.; Gong, B.; Zhao, Y.; Zhang, J.; Zheng, C.; Wu, J.C. Selective photocatalytic reduction of CO_2 into CH4 over Pt-Cu_2O TiO_2 nanocrystals: The interaction between Pt and Cu_2O cocatalysts. *Appl. Catal. B Environ.* **2017**, *202*, 695–703. [CrossRef]
20. Larrazábal, G.O.; Martín, A.J.; Krumeich, F.; Hauert, R.; Pérez-Ramírez, J. Solvothermally-Prepared Cu_2O Electrocatalysts for CO_2Reduction with Tunable Selectivity by the Introduction of p-Block Elements. *ChemSusChem* **2017**, *10*, 1255–1265. [CrossRef]
21. Munir, S.; Varzeghani, A.R.; Kaya, S. Electrocatalytic reduction of CO_2 to produce higher alcohols. *Sustain. Energy Fuels* **2018**, *2*, 2532–2541. [CrossRef]
22. Ning, H.; Wang, X.; Wang, W.; Mao, Q.; Yang, Z.; Zhao, Q.; Song, Y.; Wu, M. Cubic Cu_2O on nitrogen-doped carbon shells for electrocatalytic CO_2 reduction to C2H4. *Carbon* **2019**, *146*, 218–223. [CrossRef]
23. Gao, Y.; Wu, Q.; Liang, X.; Wang, Z.; Zheng, Z.; Wang, P.; Huang, B. Cu2O Nanoparticles with Both Facets for Enhancing the Selectivity and Activity of CO2 Electroreduction to Ethylene. *Adv. Sci.* **2020**, *7*, 1902820. [CrossRef]
24. Zhang, Y.; Zhang, X.; Chen, K.; Sun, W. Supramolecular Engineering to Improve Electrocatalytic CO_2 Reduction Activity of Cu_2O. *ChemSusChem* **2021**, *14*, 1847–1852. [CrossRef] [PubMed]
25. Jun, M.; Kwak, C.; Lee, S.Y.; Joo, J.; Kim, J.M.; Im, D.J.; Lee, K. Microfluidics-Assisted Synthesis of Hierarchical Cu_2O Nanocrystal as C_2-Selective CO_2 Reduction Electrocatalyst. *Small Methods* **2022**. [CrossRef] [PubMed]
26. Cotta, M.A. Quantum Dots and Their Applications: What Lies Ahead? *ACS Appl. Nano Mater.* **2020**, *3*, 4920–4924. [CrossRef]
27. Yin, M.; Wu, C.K.; Lou, Y.; Burda, C.; Koberstein, J.T.; Zhu, A.Y.; O'Brien, S. Copper Oxide Nanocrystals. *J. Am. Chem. Soc.* **2005**, *127*, 9506–9511. [CrossRef] [PubMed]
28. Borgohain, K.; Murase, N.; Mahamuni, S. Synthesis and properties of Cu_2O quantum particles. *J. Appl. Phys.* **2002**, *92*, 1292–1297. [CrossRef]
29. Nguyen, D.C.T.; Cho, K.Y.; Oh, W.-C. A facile route to synthesize ternary Cu_2O quantum dot/graphene-TiO_2 nanocomposites with an improved photocatalytic effect. *Fuller. Nanotub. Carbon Nanostruct.* **2017**, *25*, 684–690. [CrossRef]
30. Cui, W.; An, W.; Liu, L.; Hu, J.; Liang, Y. Novel Cu2O quantum dots coupled flower-like BiOBr for enhanced photocatalytic degradation of organic contaminant. *J. Hazard. Mater.* **2014**, *280*, 417–427. [CrossRef]
31. Xiong, Y.; Li, Z.; Zhang, R.; Xie, Y.; Yang, A.J.; Wu, C. From Complex Chains to 1D Metal Oxides: A Novel Strategy to Cu2O Nanowires. *J. Phys. Chem. B* **2003**, *107*, 3697–3702. [CrossRef]
32. Guan, L.; Pang, H.; Wang, J.; Lu, Q.; Yin, J.; Gao, F. Fabrication of novel comb-like Cu2O nanorod-based structures through an interface etching method and their application as ethanol sensors. *Chem. Commun.* **2010**, *46*, 7022–7024. [CrossRef]
33. Aref, A.; Xiong, L.; Yan, N.; Abdulkarem, A.; Yu, Y. Cu2O nanorod thin films prepared by CBD method with CTAB: Substrate effect, deposition mechanism and photoelectrochemical properties. *Mater. Chem. Phys.* **2011**, *127*, 433–439. [CrossRef]
34. Chen, R.; Wang, Z.; Zhou, Q.; Lu, J.; Zheng, M. A Template-Free Microwave Synthesis of One-Dimensional Cu2O Nanowires with Desired Photocatalytic Property. *Mater* **2018**, *11*, 1843. [CrossRef] [PubMed]
35. Yu, Y.; Du, F.P.; Yu, J.; Zhuang, Y.Y.; Wong, P.K. One-dimensional shape-controlled preparation of porous Cu2O nano-whiskers by using CTAB as a template. *J. Solid State Chem.* **2004**, *177*, 4640–4647. [CrossRef]
36. Qu, Y.; Li, X.; Chen, G.; Zhang, H.; Chen, Y. Synthesis of Cu2O nano-whiskers by a novel wet-chemical route. *Mater. Lett.* **2008**, *62*, 886–888. [CrossRef]

37. Choi, H.K.; Lee, A.; Park, M.; Lee, D.S.; Bae, S.; Lee, S.K.; Lee, S.H.; Lee, T.; Kim, T.W. Hierarchical Porous Film with Layer-by-Layer Assembly of 2D Copper Nanosheets for Ultimate Electromagnetic Interference Shielding. *ACS Nano* **2021**, *15*, 829–839. [CrossRef]
38. Kinoshita, K.; Yamada, T. A new copper oxide superconductor containing carbon. *Nature* **1992**, *357*, 313–315. [CrossRef]
39. Pawar, S.M.; Pawar, B.S.; Hou, B.; Kim, J.; Ahmed, A.T.A.; Chavan, H.S.; Jo, Y.; Cho, S.; Inamdar, A.I.; Gunjakar, J.L.; et al. Self-assembled two-dimensional copper oxide nanosheet bundles as an efficient oxygen evolution reaction (OER) electrocatalyst for water splitting applications. *J. Mater. Chem. A* **2017**, *5*, 12747–12751. [CrossRef]
40. Matencio, S.; Barrena, E.; Ocal, C. Coming across a novel copper oxide 2D framework during the oxidation of Cu(111). *Phys. Chem. Chem. Phys.* **2016**, *18*, 33303–33309. [CrossRef]
41. Yin, K.; Zhang, Y.Y.; Zhou, Y.; Sun, L.; Chisholm, M.F.; Pantelides, S.T.; Zhou, W. Unsupported single-atom-thick copper oxide monolayers. *2D Mater.* **2016**, *4*, 011001. [CrossRef]
42. Lee, S.; Wang, S.; Wern, C.; Yi, S. The Green Synthesis of 2D Copper Nanosheets and Their Light Absorption. *Mater* **2021**, *14*, 1926. [CrossRef]
43. Luc, W.; Fu, X.; Shi, J.; Lv, J.J.; Jouny, M.; Ko, B.H.; Xu, Y.; Tu, Q.; Hu, X.; Wu, J.; et al. Two-dimensional copper nanosheets for electrochemical reduction of carbon monoxide to acetate. *Nat. Catal.* **2019**, *2*, 423–430. [CrossRef]
44. Mallik, M.; Monia, S.; Gupta, M.; Ghosh, A.; Toppo, M.P.; Roy, H. Synthesis and characterization of Cu2O nanoparticles. *J. Alloys Compd.* **2020**, *829*, 154623. [CrossRef]
45. Amaniampong, P.N.; Trinh, Q.T.; Wang, B.; Borgna, A.; Yang, Y.; Mushrif, S.H. Frontispiece: Biomass Oxidation: Formyl C-H Bond Activation by the Surface Lattice Oxygen of Regenerative CuO Nanoleaves. *Angew. Chem. Int. Ed.* **2015**, *54*, 8928–8933. [CrossRef] [PubMed]
46. Bhattacharjee, A.; Begum, S.; Neog, K.; Ahmaruzzaman, M. Facile synthesis of 2D CuO nanoleaves for the catalytic elimination of hazardous and toxic dyes from aqueous phase: A sustainable approach. *Environ. Sci. Pollut. Res.* **2016**, *23*, 11668–11676. [CrossRef] [PubMed]
47. Xu, H.; Wang, A.W.; Zhu, W. Shape Evolution and Size-Controllable Synthesis of Cu2O Octahedra and Their Morphology-Dependent Photocatalytic Properties. *J. Phys. Chem. B* **2006**, *110*, 13829–13834. [CrossRef] [PubMed]
48. Mirmotallebi, M.; Zad, A.I.; Hosseini, Z.S.; Jokar, E. Characterization of three-dimensional reduced graphene oxide/copper oxide heterostructures for hydrogen sulfide gas sensing application. *J. Alloys Compd.* **2018**, *740*, 1024–1031. [CrossRef]
49. Yu, L.; Jin, Y.; Li, L.; Ma, J.; Wang, G.; Geng, B.; Zhang, X. 3D porous gear-like copper oxide and their high electrochemical performance as supercapacitors. *CrystEngComm* **2013**, *15*, 7657–7662. [CrossRef]
50. Fei, X.; Shao, Z.; Chen, X. Synthesis of hierarchical three-dimensional copper oxide nanostructures through a biomineralization-inspired approach. *Nanoscale* **2013**, *5*, 7991–7997. [CrossRef]
51. Shinde, S.K.; Dubal, D.P.; Ghodake, G.S.; Fulari, V.J. Hierarchical 3D-flower-like CuO nanostructure on copper foil for supercapacitors. *RSC Adv.* **2015**, *5*, 4443–4447. [CrossRef]
52. Karthikeyan, S.; Ahmed, K.; Osatiashtiani, A.; Lee, A.F.; Wilson, K.; Sasaki, K.; Coulson, B.; Swansborough-Aston, W.; Douthwaite, R.E.; Li, W. Pompon Dahlia-like Cu_2O/rGO Nanostructures for Visible Light Photocatalytic H_2 Production and 4-Chlorophenol Degradation. *ChemCatChem* **2020**, *12*, 1699–1709. [CrossRef]
53. Gou, L.; Murphy, C.J. Solution-Phase Synthesis of Cu2O Nanocubes. *Nano Lett.* **2002**, *3*, 231–234. [CrossRef]
54. Kuo, C.H.; Huang, M.H. Facile Synthesis of Cu2O Nanocrystals with Systematic Shape Evolution from Cubic to Octahedral Structures. *J. Phys. Chem. C* **2008**, *112*, 18355–18360. [CrossRef]
55. Wan, L.; Zhou, Q.; Wang, X.; Wood, T.E.; Wang, L.; Duchesne, P.N.; Guo, J.; Yan, X.; Xia, M.; Li, Y.F.; et al. Cu2O nanocubes with mixed oxidation-state facets for (photo)catalytic hydrogenation of carbon dioxide. *Nat. Catal.* **2019**, *2*, 889–898. [CrossRef]
56. Ji, Y.; Luo, Y. Theoretical Study on the Mechanism of Photoreduction of CO2 to CH4 on the Anatase TiO2(101) Surface. *ACS Catal.* **2016**, *6*, 2018–2025. [CrossRef]
57. Yin, G.; Nishikawa, M.; Nosaka, Y.; Srinivasan, N.; Atarashi, D.; Sakai, E.; Miyauchi, M. Photocatalytic Carbon Dioxide Reduction by Copper Oxide Nanocluster-Grafted Niobate Nanosheets. *ACS Nano* **2015**, *9*, 2111–2119. [CrossRef] [PubMed]
58. An, X.; Li, K.; Tang, J. Cu2O/reduced graphene oxide composites for the photocatalytic conversion of CO2. *ChemSusChem* **2014**, *7*, 1086–1093. [CrossRef]
59. Ovcharov, M.; Mishura, A.; Shcherban, N.; Filonenko, S.; Granchak, V. Photocatalytic reduction of CO2 using nanostructured Cu2O with foam-like structure. *Sol. Energy* **2016**, *139*, 452–457. [CrossRef]
60. Wang, J.C.; Zhang, L.; Fang, W.X.; Ren, J.; Li, Y.Y.; Yao, H.C.; Wang, J.S.; Li, Z.J. Enhanced photoreduction CO_2 activity over direct Z-scheme α-Fe_2O_3/Cu_2O heterostructures under visible light irradiation. *ACS Appl. Mater. Interfaces* **2015**, *7*, 8631–8639. [CrossRef]
61. Kim, C.; Cho, K.M.; Al-Saggaf, A.; Gereige, I.; Jung, H.T. Z-scheme photocatalytic CO2 conversion on three-dimensional BiVO4/carbon-coated Cu2O nanowire arrays under visible light. *ACS Catal.* **2018**, *8*, 4170–4177. [CrossRef]
62. Li, X.; Wei, D.; Ye, L.; Li, Z. Fabrication of Cu2O-RGO/BiVO4 nanocomposite for simultaneous photocatalytic CO2 reduction and benzyl alcohol oxidation under visible light. *Inorg. Chem. Commun.* **2019**, *104*, 171–177. [CrossRef]
63. Chang, P.Y.; Tseng, I.H. Photocatalytic conversion of gas phase carbon dioxide by graphitic carbon nitride decorated with cuprous oxide with various morphologies. *J. CO2 Util.* **2018**, *26*, 511–521. [CrossRef]

64. Aguirre, M.E.; Zhou, R.; Eugene, A.J.; Guzman, M.I.; Grela, M.A. Cu2O/TiO2 heterostructures for CO2 reduction through a direct Z-scheme: Protecting Cu_2O from photocorrosion. *Appl. Catal. B Environ.* **2017**, *217*, 485–493. [CrossRef]
65. Zhang, F.; Li, Y.H.; Qi, M.Y.; Tang, Z.R.; Xu, Y.J. Boosting the activity and stability of Ag-Cu2O/ZnO nanorods for photocatalytic CO2 reduction. *Appl. Catal. B Environ.* **2020**, *268*, 118380. [CrossRef]
66. Lum, Y.; Ager, J.W. Stability of Residual Oxides in Oxide-Derived Copper Catalysts for Electrochemical CO2 Reduction Investigated with 18O Labeling. *Angew. Chem. Int. Ed.* **2018**, *57*, 551–554. [CrossRef] [PubMed]
67. Hori, Y.; Kikuchi, K.; Suzuki, S. Production of Co and Ch4in Electrochemical Reduction of Co2at Metal Electrodes in Aqueous Hydrogencarbonate Solution. *Chem. Lett.* **1985**, *14*, 1695–1698. [CrossRef]
68. Kim, J.; Choi, W.; Park, J.W.; Kim, C.; Kim, M.; Song, H. Branched Copper Oxide Nanoparticles Induce Highly Selective Ethylene Production by Electrochemical Carbon Dioxide Reduction. *J. Am. Chem. Soc.* **2019**, *141*, 6986–6994. [CrossRef]
69. Zhao, Y.; Wang, C.; Wallace, G.G. Tin nanoparticles decorated copper oxide nanowires for selective electrochemical reduction of aqueous CO2 to CO. *J. Mater. Chem. A* **2016**, *4*, 10710–10718. [CrossRef]
70. Qiao, J.; Liu, Y.; Hong, F.; Zhang, J. A review of catalysts for the electroreduction of carbon dioxide to produce low-carbon fuels. *Chem. Soc. Rev.* **2014**, *43*, 631–675. [CrossRef]
71. Dattila, F.; García-Muelas, R.; López, N. Active and Selective Ensembles in Oxide-Derived Copper Catalysts for CO2 Reduction. *ACS Energy Lett.* **2020**, *5*, 3176–3184. [CrossRef]
72. Xiao, H.; Goddard, W.A.; Cheng, T.; Liu, Y. Cu metal embedded in oxidized matrix catalyst to promote CO_2 activation and CO dimerization for electrochemical reduction of CO_2. *Proc. Natl. Acad. Sci. USA* **2017**, *114*, 6685–6688. [CrossRef]
73. Nitopi, S.; Bertheussen, E.; Scott, S.B.; Liu, X.; Engstfeld, A.K.; Horch, S.; Seger, B.; Stephens, I.E.L.; Chan, K.; Hahn, C.; et al. Progress and Perspectives of Electrochemical CO2 Reduction on Copper in Aqueous Electrolyte. *Chem. Rev.* **2019**, *119*, 7610–7672. [CrossRef]
74. Jiang, K.; Sandberg, R.B.; Akey, A.J.; Liu, X.; Bell, D.; Nørskov, J.K.; Chan, K.; Wang, H. Metal ion cycling of Cu foil for selective C–C coupling in electrochemical CO2 reduction. *Nat. Catal.* **2018**, *1*, 111–119. [CrossRef]
75. Jung, H.; Lee, S.Y.; Lee, C.W.; Cho, M.K.; Won, D.H.; Kim, C.; Oh, H.S.; Min, B.K.; Hwang, Y.J. Electrochemical Fragmentation of Cu_2O Nanoparticles Enhancing Selective C–C Coupling from CO_2 Reduction Reaction. *J. Am. Chem. Soc.* **2019**, *141*, 4624–4633. [CrossRef] [PubMed]
76. Mandal, L.; Yang, K.R.; Motapothula, M.R.; Ren, D.; Lobaccaro, P.; Patra, A.; Sherburne, M.; Batista, V.S.; Yeo, B.S.; Ager, J.W.; et al. Investigating the Role of Copper Oxide in Electrochemical CO_2 Reduction in Real Time. *ACS Appl. Mater. Interfaces* **2018**, *10*, 8574–8584. [CrossRef] [PubMed]
77. Roy, A.; Jadhav, H.S.; Gil Seo, J. Cu_2O/CuO Electrocatalyst for Electrochemical Reduction of Carbon Dioxide to Methanol. *Electroanalysis* **2020**, *33*, 705–712. [CrossRef]
78. Li, M.; Tian, X.; Garg, S.; Rufford, T.E.; Zhao, P.; Wu, Y.; Yago, A.J.; Ge, L.; Rudolph, V.; Wang, G. Modulated Sn Oxidation States over a Cu_2O-Derived Substrate for Selective Electrochemical CO_2 Reduction. *ACS Appl. Mater. Interfaces* **2020**, *12*, 22760–22770. [CrossRef]
79. Zhan, C.; Dattila, F.; Rettenmaier, C.; Bergmann, A.; Kühl, S.; García-Muelas, R.; Cuenya, B.R. Revealing the CO Coverage-Driven C–C Coupling Mechanism for Electrochemical CO_2 Reduction on Cu_2O Nanocubes via Operando Raman Spectroscopy. *ACS Catal.* **2021**, *11*, 7694–7701. [CrossRef]
80. Li, C.W.; Kanan, M.W. CO_2 Reduction at Low Overpotential on Cu Electrodes Resulting from the Reduction of Thick Cu_2O Films. *J. Am. Chem. Soc.* **2012**, *134*, 7231–7234. [CrossRef]
81. Yan, C.; Luo, W.; Yuan, H.; Liu, G.; Hao, R.; Qin, N.; Wang, Z.; Liu, K.; Wang, Z.; Cui, D.; et al. Stabilizing intermediates and optimizing reaction processes with N doping in Cu_2O for enhanced CO_2 electroreduction. *Appl. Catal. B Environ.* **2022**, *308*, 121191. [CrossRef]
82. Liu, J.; Cheng, L.; Wang, Y.; Chen, R.; Xiao, C.; Zhou, X.; Li, C. Dynamic determining Cu+ roles for CO_2 reduction on electrochemically stable Cu_2O based nanocubes. *J. Mater. Chem. A* **2022**, *10*, 8459–8465. [CrossRef]
83. Luo, H.; Li, B.; Ma, J.G.; Cheng, P. Surface Modification of Nano-Cu_2O for Controlling CO_2 Electrochemical Reduction to Ethylene and Syngas. *Angew. Chem. Int. Ed.* **2022**, *61*, e202116736. [CrossRef]